Astron. Astrophys. 319, 948–966 (1997)

ASTRONOMY
AND
ASTROPHYSICS

# Magnitude and color distribution of background stars as a probe of small-scale structure in the spatial distribution of interstellar dust⋆

**S. Thoraval**[1], **P. Boissé**[1], **and G. Duvert**[2]

[1] Radioastronomie, UA CNRS 336, Ecole Normale Supérieure, 24, rue Lhomond, F-75231 Paris Cedex 05, France
[2] Laboratoire d'Astrophysique, Observatoire de Grenoble, B.P. 53X, F-38041 Grenoble Cedex, France

Received 18 December 1995 / Accepted 1 March 1996

**Abstract.** In order to determine the amplitude of small scale fluctuations of the extinction induced by molecular material, we have reconsidered the star count method in the context of fragmented clouds. We show that by studying the full magnitude distribution it is possible not only to estimate extinctions in a more reliable way than by using the classical procedure, but also to derive constraints on cloud structure at very small scales (down to few $\mu$arcsec). This technique has been applied to a low latitude cloud located at a distance of about 200 pc in the IC 5146 complex. Analyses of CCD B, V, R, i photometric data on more than one thousand stars indicate that the cloud extinction is close to uniform over the 45 arcmin$^2$ field.

To better constrain the fluctuations of the extinction, the distribution of the colors of background stars is considered. Analysis of the V − i data implies that variations are present but at a level no larger than $\sigma(A_V)/A_V \approx 25\%$. The accurate $42''$ (corresponding to 0.04 pc) resolution map of the V − i color excess obtained indicates that most of these variations occur at scales larger than $\approx$ 1 arcmin. We therefore conclude that the contribution of small scales to extinction fluctuations is quite small and that, at these scales, molecular material behaves as if it were homogeneous regarding the transfer of continuum UV radiation.

A comparison of our extinction data with a high resolution map of the same field in the $J = 1$–0 and $J = 2$–1 CO lines shows a complete absence of correlation between $A_V$ and $I$(CO) at these small scales, which implies an upper limit for the $H_2$–$I$(CO) conversion factor (defined as $\delta N(H_2)/\delta I(CO)$) of about $10^{19}$ $H_2$ molecules cm$^{-2}$/K km s$^{-1}$. We discuss the implications of this lack of correlation on the structure of molecular clouds and on the origin of the large spatial variability displayed by CO emission.

**Key words:** dust, extinction – ISM: clouds, structure, molecules – ISM: IC 5146

## 1. Introduction

In the two past decades, a lot of evidences has accumulated indicating that the bulk of the material contained inside molecular clouds is not distributed uniformly in space (we shall not be concerned here with high density cores which represent a small fraction of the total mass). A first argument is that if gas were spread uniformly within clouds, mass and size estimates would imply a density which is well below the value required for efficient collisional excitation of CO molecules (Blitz & Shu 1980). Detailed studies attempting to reproduce the overall characteristics of CO isotopomers emission (line intensity ratios, line profiles, etc) strongly suggest the presence of discrete emitting cells (Goldsmith et al. 1975, Baker 1976, Martin et al. 1984, Falgarone et al. 1992). Further, the presence of dense clumps with a small volume filling factor moving in a low density phase is a means to avoid the short dissipation time-scale problem raised by the large velocity dispersions observed (the original motivation of Kwan & Sanders 1986). At large and intermediate scales, the fragmented character of the $^{12}$CO, $^{13}$CO emitting gas is very clearly apparent in maps obtained using millimeter wave techniques (Pérault et al. 1985; Bally et al. 1987).

However, individual fragments have not yet shown up in high spectral resolution and good signal to noise velocity profiles, a paradoxical fact which can be used to place tight constraints on their number density and size. Thus, from the smoothness of CO spectra, Tauber et al. (1991) get a lower limit of $\approx 10^4$ in a 45 arcsec beam towards Orion. Using a similar reasoning and given the uniformity of line intensity ratio between the two first rotational lines of CO, Falgarone & Phillips (1996) find an upper limit of 50 AU for the size of the CO-rich dense fragments at a cloud's edge. The existence of structures at still

*Send offprint requests to*: S. Thoraval

⋆ Based on observations made at Observatoire de Haute-Provence (France, operated by the CNRS), Observatoire du Pic du Midi and at the 30m IRAM telescope (Pico Veleta, Spain)

smaller scales has been investigated through variability studies. From the detection of secular changes in the $H_2CO$ absorption profile toward NRAO 150 and 3C111, Marscher et al. (1993) suggest the existence of AU-scale clumps inside molecular clouds (see also Moore & Marscher 1995). Very interesting constraints can also be drawn from the comparison of the absorption profile of CO against a compact continuum source and the profile of the CO emission in a large beam pointing towards the same direction. The close similarity and smoothness of both line profiles imply again that a large number of clumps are intersected by the line of sight. Thus, Marscher et al. (1991) get a lower limit of 70 CO absorbing fragments; since the amount of intervening material is quite moderate ($A_V \approx 1.$), this corresponds to a very low upper limit for the extinction induced by individual clumps. In addition, these observations show that the CO gas intersected by an "ideal" line of sight samples surprisingly well the velocity field of the whole material comprised within the beam.

Further indirect evidence against homogeneity is provided by observations of ionized or atomic carbon fine-structure lines and high J CO lines. Observations of the M17 SW region showed that the CII 158 $\mu$m emission is very extended around the HII region (Stutzki et al. 1988), a feature that appeared later to be shared by other bright CII sources illuminated by massive young stars (Stacey et al. 1993) as well as by CI 609 $\mu$m sources (Phillips & Huggins 1981; Keene et al. 1985). The most realistic explanation for the large extent of the CI and CII emission appears to be the existence of a clumpy structure in the photodissociation region (Stutzki et al. 1988; Meixner & Tielens 1993). Subsequent mapping of the M17 and Orion sources in the CO lines did confirm the presence of a clumpy structure in these photodissociation regions (Stutzki & Güsten, 1990; Tauber et al. 1994).

The above studies indicate that non uniformity may be a generic property of interstellar (and in particular molecular) matter, irrespective of the type of cloud (star-forming or quiescent) concerned. The presence of pronounced structure should then have considerable impact on the physics and chemistry of interstellar matter and therefore on most of its observational properties. In this regard, the UV radiation field is a key parameter since it is expected to decrease much less rapidly towards the interior of the cloud when density fluctuations are present. Detailed calculations have been performed which allow to quantitatively describe the transfer of continuum radiation inside two-phase or N-phase clouds (Boissé 1990; Hobson & Scheuer 1993; Spaans 1996; Witt & Gordon 1996). Modelling of the chemistry in such clumpy media confirms that fragmentation has a major effect on the expected line intensities from the most abundant species (Spaans 1996).

One major limitation encountered when attempting to use the above results in order to model real (i.e. non-uniform) molecular clouds and understand specific observations is that we do not know yet how the structure is to be properly described. The studies already carried out allow to quantify the dependence of various cloud characteristics on internal structure and show that several observed properties which homogeneous models failed to explain can be reproduced when clumpy clouds are considered. But they can hardly be used to infer the structure since even the simplest two-phase models require the introduction of three additional parameters with respect to uniform models (e.g. the clump opacity, the clump filling factor and clump/interclump density contrast). Further, the latter are in general not related in a univocal way to observable properties. This is clearly an uncomfortable situation and searching for acceptable fits among such a vast range of models without any restriction may be very misleading. Indeed, one may thus attribute to clumpiness discrepancies between observations and predictions from homogeneous models which are in fact due to other reasons, e.g. to an inadequate treatment of the physical processes involved.

A few attempts have been made to determine from CO observations themselves, the filling factor of dense gas or the clump/interclump density ratio (cf Bally et al. 1987). First, there is no general agreement about the actual value of the latter parameters. Second, in the models built to analyse observations of clumpy regions, it is the spatial distribution of the dust which is of primary importance because the latter governs the penetration of the radiation. Extracting structural parameters from CO observations could lead to erroneous values. Indeed, although CO emission exhibits a "quasi-homogeneous" behavior at the scale of a giant molecular cloud (Castets et al. 1990), it is by no way obvious that at small scales, there still exists a simple relationship between the intensity of CO isotopomers emission and the amount of $H_2$ molecules and dust (effects of time-dependent chemistry, selective photodissociation, averaging over the beam or simply radiative transfer in the CO millimeter lines could tend to erase the correlation observed at large scales between $I$(CO) and $A_V$ which may result in a large scatter of the local $N(H_2)/I(CO)$ conversion factor).

It is then highly desirable to characterize the spatial distribution of dust in a direct way, especially at small scales where very little information is available. If a large fraction of the dust were enclosed in tiny opaque fragments, the effective opacity would not be determined solely by the amount of dust but also, and possibly primarily, by its spatial distribution (Boissé, 1990). It is clearly essential to determine if this is actually the case or if instead, clouds globally behave like a homogeneous medium, at least below some scale. Beyond this basic question, it is critical for modelling to know whether the effective opacity is determined by the densest regions or by the interclump phase. The existence and strength of spatial structure in the extinction is also of importance in several other questions such as the correction to be applied for the dimming of distant extragalactic objects by foreground galactic dust (the estimates derived from large beam HI or CO measurements could be much affected if structure within the beam is present) or studies of the large scale distribution of galaxies (Seldner & Uson 1983).

Studies of the dust distribution have already been performed using multi-band Strömgren photometry of individuals B, A and F stars (see e.g. Knude 1979, Franco 1995), star counts or far infrared (FIR) data, especially those provided by the IRAS satellite. The first method only provides a loose sampling of the region considered while the two latter are restricted to an

angular resolution of a few arcminutes (0.1 pc for a nearby cloud at a distance of 100 pc) which may not be good enough to give a representative picture of the actual distribution, given the very small sizes of fragments inferred from molecular line studies. Star counts have been widely used to measure extinctions, with the motivation that this parameter may be a good tracer of the total mass, i.e. of molecular hydrogen (see Dickman 1978 and, for the extension of the method in the near infrared, Lada et al. 1994). In the presence of fluctuations within individual count cells, this method only yields an "apparent opacity". The latter quantity is no longer proportional to the column density of grains and just gives a lower limit to the average value (Boissé, 1990). If density fluctuations are large, star counts may then considerably underestimate the true amount of dust.

Far infrared emission is less subject to these problems since at 60 or 100 $\mu$m, the opacity is expected to be small; therefore, even in the presence of unresolved structure, IRAS measurements still provides the average intensity. However, although these data are a unique tool for studies of the overall cloud morphology, they cannot be used as an unambiguous indicator of the dust content because the heating rate varies locally along the line of sight. Thus, the FIR brightness of a spherical cloud is not expected to increase linearly with opacity (see Fig. 9 in Bernard et al. 1992). In other words, the dust particles which give the major contribution to the extinction are not necessarily those which emit most of the FIR radiation, grains being spread over a broad range of temperatures which is poorly sampled by observations at 60 and 100 $\mu$m (Pajot et al. 1986). This is well illustrated by the fact that a slightly different cloud morphology shows up when using either the 60 $\mu$m, 100 $\mu$m data or a combination of both appropriate to select preferentially the cold dust component (Abergel et al. 1994). The statistical analysis of the FIR brightness distribution performed by Gautier et al. (1992) for large complexes indicates that most of the structure is contained in large scales and lead, when extrapolated at small scales (below the IRAS resolution) to small expected column density fluctuations. However, the analysis involves a large region and gives much weight to the diffuse atomic regions which cover most of the area studied. The higher shielding mentioned above for the molecular regions further tends to reduce the weight of the latter. Therefore, one cannot exclude on the basis of these results alone, the existence of a new regime for molecular regions, with additional power at small scales associated to the CO emitting fragments discussed above. Some of the problems met with the interpretation of the FIR measurements problem could be circumvented by performing observations in the submillimeter range where the intensity depends less strongly on the grain temperature but these data still remain difficult to obtain, especially at high spatial resolutions and for quiescent clouds with low or intermediate opacity.

We have undertaken a study of small scale structure in the extinction suffered by various background objects (stars, HII regions, galaxies) and induced by local molecular material with moderate opacity. Extinction as an indicator of dust column density has two important advantages. First, insofar as dust is a good tracer of atomic and molecular hydrogen (Bohlin et al. 1978; note that the scatter around the linear relation given by these authors is relatively small), extinction can provide information on the spatial distribution of the total mass down to extremely small scales. Second, studies of the optical extinction allow to investigate in a very direct way whether or not the transfer of optical photons is affected by the presence of a fragmented small scale structure. In a previous paper (Thoraval et al. 1996) we performed a sensitive search for AU-scale fluctuations in the extinction towards stars with foreground material by investigating the variability of their broad-band magnitudes. We obtained a stringent upper limit which indicates that the AU-scale structure inferred by Marscher et al. (1993) from $H_2CO$ absorption measurements is not density structure but more likely reflects spatial variability in either the relative abundance or excitation of this species.

In this paper, we generalize the classical star counts to non-uniform clouds and show how the use of both multi-color CCD photometric data and modern automated detection procedures allows to efficiently probe the structure of a foreground cloud at all scales smaller than the field size, including extremely small ones (Sect. 2). This point is illustrated by observations of a low galactic latitude translucent cloud (Sect. 3). Complementary optical spectroscopic data have been acquired to obtain independent determinations of the extinction towards selected stars in these fields (Sect. 4). We also present in Sect. 5 high angular resolution millimeter wave $^{12}CO$ observations of this cloud. Since we could get quite detailed information on the distribution of the dust, we then compare the behaviour of $^{12}CO$ emission and extinction as mass tracers. Finally, the implications of our results regarding the structure of molecular clouds are discussed in Sect. 6 and summarized in Sect. 7.

## 2. Star counts and inhomogeneous clouds

The value of background stars in the context of cloud structure stems from the fact that they define extremely narrow beams with an angular extent of no more than $\approx 5$ $\mu$arcsec (for a solar type star assumed at 1 kpc). Provided that their contribution to the total column density is not too small, clumps with this size or larger will then not be smeared out as they would for observations implying averaging over a large 3D volume (as in the radio range for instance).

Before discussing the behaviour of star counts through clumpy clouds, let us recall first the principles of the procedure commonly used to measure extinctions and outline the main underlying assumptions.

### *2.1. The classical star count technique*

The conventional method consists in comparing the integrated number of stars within a given cell toward the cloud and in a nearby reference field free from extinction (Bok and Cordwell, 1973; Dickman, 1978). Other procedures involving differential counts have also been proposed. Although they allow in principle to determine the distance of the cloud, they are rarely used

because of practical difficulties: 1) the method requires a measurement of the star magnitudes which is not straightforward on photographic plates; 2) the number of stars per magnitude interval is small which results in poor statistics. The determination of the extinction $A$ from the integrated surface densities of stars, $N_c(< m)$ and $N_r(< m)$ (hereafter noted $N_c(m)$ and $N_r(m)$) for the cloud and reference fields respectively, relies on three assumptions:

- the population of stars background to the cloud is similar to that in the reference field (i.e. $N_c = N_r$ if $A = 0$),
- $A$ is uniform over the count cell,
- $N_r(m)$ follows an exponential law with $\log(N_r(m)) = a+bm$. Then, $\log(N_c)$ follows a similar law ($\log(N_c(m)) = a+b(m-A)$) and $A$ is provided by the expression,

$$A = -\frac{1}{b}\log\left(\frac{N_c(m)}{N_r(m)}\right) . \quad (1)$$

The above formula also requires that all stars are located behind the cloud but this condition is satisfactorily fulfilled for nearby clouds ($d \approx$ a few 100 pc). In this method, no spatial variation of $A$ can be seen at scales below the cell size. Rossano (1980) has discussed in detail the effects due to fluctuations of $A$ across the sampling element. If the number of stars per cell is large enough, the presence of strong systematic gradients at scales comparable to the cell size may result in an apparent non random distribution of the star positions within the cell. On the opposite, extinction variations of a stochastic nature may be completely unrecognizable.

In order to illustrate some ideas or methods developed in this paper, it will be convenient to consider a few very simple inhomogeneous models. Model referred to as "C" (for clumpy) in the following corresponds to a cloud made of totally opaque clumps covering a fraction $f$ of the surface ($f$ is assumed to be spatially uniform) with no material in between. Then, the extinction $A$ through the cloud is either infinite (probability: $f$) or 0 (probability: $1-f$). A more general case (model "CH", for Clumpy-Homogeneous) is that of a non-empty interclump phase, for which $A$ is either infinite or equals $A_0$. Note that model CH includes model C (for which $A_0 = 0$) and homogeneous models, hereafter model H ($f = 0$). In models C or CH, if the angular size subtended by a clump is comparable to or smaller than the typical separation between neighboring stars, the field will be undistinguishable from one extinguished by a homogeneous cloud. We show in the next section that, even in such a case, the full magnitude distribution of the background stars does provide information on the obscuring cloud's structure.

### *2.2. The magnitude distribution of extinguished stars*

#### 2.2.1. The general case (any cloud structure and $N_r$)

Let $N'_r(m)$ and $N'_c(m)$ be the differential magnitude distribution for stars in the reference and cloud field respectively (i.e. $N' = dN/dm$). If all stars are background to the obscuring cloud $N_c$ is related to $N_r$ through

$$N_c(m) = \int_0^\infty p(A)N_r(m-A)dA \quad (2)$$

where $p(A)$ is the fraction of the cloud projected area with an extinction $A$. This relation directly follows from the fact that the magnitude of background stars and $A$ values are uncorrelated. In model CH for instance, $p(A)$ writes $f\delta(A-A_\infty) + (1-f)\delta(A-A_0)$, where $A_\infty$ is an arbitrarily large value. Relation (2) has already been given by Rossano (1980) and holds both for the differential and integrated magnitude distributions. It implicitly assumes that stars background to the cloud studied are distributed at random on the sky and therefore provides an unbiased sampling of A values (it would seem that completely opaque fragments are missed since no star can be seen through them but this is not true as discussed later in Sect. 3.4). It is clearly seen in relation (2) that $N_c$ depends solely on $p(A)$ and does not involve any other characteristics of the spatial distribution of the extinction (such as spatial correlations). Variations of $A$, either regular or stochastic and with any scale between the field size and the extent of background stellar disks (typically a few $\mu$arcsec as quoted above), will leave the same imprint on $N_c$.

We shall not discuss here how relation (2) can be inverted to get $p(A)$. In practice, when considering real data with limited signal to noise ratio on $N_c$ and $N_r$, it is more convenient to start from a given $p(A)$ in parametric form and use observations to constrain the acceptable range for the model parameters. When applying the method, our purpose will then be to determine $N_r$ and $N_c$ as accurately as possible and use relation (2) to characterize or at least constrain the fluctuations of $A$.

#### 2.2.2. Exponential form for $N_r$

It is straightforward to establish that if $N_r$ writes $10^{(a+bm)}$, $N_c$ display a similar form and is given by the expression

$$N_c(m) = 10^{(a-bA')+bm} = N_r(m)10^{-bA'} \quad (3)$$

$$\text{with } A' = -\frac{1}{b}\log(\langle 10^{-bA}\rangle)$$

$$\text{where } \langle 10^{-bA}\rangle = \int_0^\infty p(A)10^{-bA}dA .$$

$A'$ is an "apparent extinction", i.e. the extinction of the uniform cloud that would yield the same $N_c(m)$. Similarly, one can define an "apparent opacity",

$$\tau' = -\frac{1}{2.5b}\mathrm{Ln}(\langle e^{-2.5b\tau}\rangle) .$$

As discussed by Boissé (1990), when $b = 0.4$, $\tau'$ coincides with the effective opacity which is directly related to the average tranparency of the medium (if $b \neq 0.4$, $\tau'$ keeps the same physical meaning of an average with much weight given to the

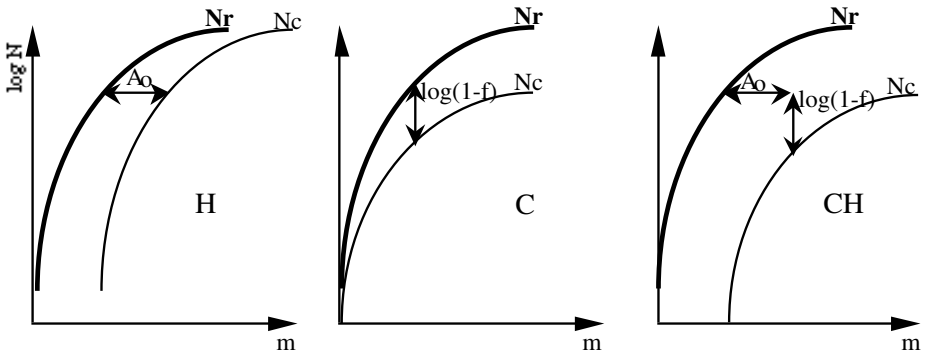


**Fig. 1.** Magnitude distributions expected in a field extinguished by a homogeneous cloud (H; extinction $A_0$), a clumpy cloud (C; clump surface covering factor: $f$) or a cloud made of clumps embedded in a low density phase (CH: see text)

regions of low opacity). We recall that the effective opacity, $\tau_{\rm eff}$, and effective extinction, $A_{\rm eff}$, are defined by

$$\tau_{\rm eff} = -{\rm Ln}(\langle e^{-\tau}\rangle) \quad \text{and} \quad A_{\rm eff} = -2.5\log(\langle 10^{-\frac{A}{2.5}}\rangle) \; .$$

It is remarkable that for $N_{\rm r}\alpha 10^{(a+bm)}$, the effect of the cloud is entirely contained in one single quantity, $A'$. An immediate consequence is that such a case is highly degenerated: many distinct cloud models are associated with the same $A'$ (and thus $N_{\rm c}$) and cannot be distinguished. Hence, the use of magnitude distributions to constrain cloud structure will heavily rely upon the curvature displayed by $\log(N_{\rm r})$ (cf Sect. 3.4).

#### 2.2.3. Model CH

Relation (2) becomes

$$N_{\rm c}(m) = (1-f)N_{\rm r}(m-A_0) \; . \tag{4}$$

The curve for $\log(N_{\rm c})$ is then obtained from that for the reference field by shifting the latter horizontally (by $\Delta m = A_0$) and vertically (by $\Delta\log(N) = \log(1-f)$). For a uniform cloud (with $f = 0$), the shift is purely horizontal while for a clumpy one (model C: $A_0 = 0$), it is purely vertical (Fig. 1). Model CH illustrates very clearly the degeneracy occuring when $N_{\rm r}\alpha 10^{(a+bm)}$. Indeed, since $\log(N)$ is linear with respect to $m$, horizontal, vertical or oblique shifts in a ($m$, $\log(N)$) diagram are equivalent. Thus, it is for instance not possible to distinguish models H, C and CH because all produce the same $N_{\rm c}$ provided $bA_0({\rm H}) = -\log(1-f({\rm C})) = bA_0({\rm CH}) - \log(1-f({\rm CH}))$.

#### 2.2.4. Methods to measure the extinction of uniform clouds

A few remarks can be made concerning the classical procedure employed to determine $A$ within the assumption of a uniform cloud. For $f = 0$, relation (4) reduces to

$$N_{\rm c}(m) = N_{\rm r}(m-A_0) \; . \tag{5}$$

Using relation (5) to determine the extinction of a uniform cloud requires the measurement of the magnitude of all stars in the field while the standard star count method is based entirely on the values $N_{\rm c}(m_{\rm l})$ and $N_{\rm r}(m_{\rm l})$, where $m_{\rm l}$ is the plate limit. However, the former procedure is by far superior to the second one because it is valid whatever the shape of $N_{\rm r}$. On the contrary, the standard star count method can be significantly affected if the adopted $b$ value (generally inferred from Van Rhijn tables) is wrong or if $N_{\rm r}(m)$ departs from an exponential law. As shown in Sect. 3, deviations from such a law do exist in reality, which is no surprise since the latter is expected to hold only for a uniform and spatially unlimited population of stars, the anticipated slope being then $b = 0.6$. The variations of both the number density and average type of stars along the line of sight tend to induce departures and reduce the average slope of the counts to $b \approx 0.2 - 0.4$.

Another important difference between the two methods is that the one based on relation (5) involves data for the cloud and reference fields that cover different magnitude intervals. Deeper observations in the cloud field are required and more precisely, optimal use of the data is achieved when $m_{\rm lim,c} = m_{\rm lim,r} + A_0$, where $m_{\rm lim,c}$ and $m_{\rm lim,r}$ are the limiting magnitudes attained for the cloud and reference fields respectively.

### *2.3. The color dependence of the counts*

Another interesting property of star counts in our context is their dependence on wavelength. To discuss this point, let us assume for simplicity that $\log(N_{\rm r})$ follows a linear law and consider observations in two different bands (say V and I for instance). For a uniform cloud, the extinction estimates provided by star counts are unbiased and the ratio of values in the V and I bands, $R_{\rm VI} = A_{\rm V}/A_{\rm I}$, is directly determined by the extinction law (i.e. the optical properties of dust grains). On the contrary, when seen through a model CH cloud, stars located behind opaque clumps are removed from the counts whatever the band considered; one therefore expects a different behaviour. The apparent extinction provided by star counts is

$$A'({\rm CH}) = A_0 - \frac{1}{b}\log(1-f)$$

from which we get

$$R'_{\rm VI} = \frac{A'_{\rm V}}{A'_{\rm I}} = \frac{A_{0,{\rm V}} - \frac{\log(1-f)}{b_{\rm V}}}{A_{0,{\rm I}} - \frac{\log(1-f)}{b_{\rm I}}}$$

where $b_{\rm V}$ and $b_{\rm I}$ are the slope of the V and I counts respectively. Since $A_{0,{\rm V}}/A_{0,{\rm I}}$ is larger than $b_{\rm I}/b_{\rm V}$ (the limit attained for a C

cloud with $A_{0,\mathrm{V\ or\ I}} = 0$), $R'_{\mathrm{VI}}$ will always be less than the true ratio $R_{\mathrm{VI}}$. Thus, the wavelength dependence of the extinction appears to be reduced. Such an effect is similar to that described by Natta and Panagia (1984) for extended sources (e.g. HII regions) seen through non-uniform clouds. In realistic cases, $b_{\mathrm{I}}/b_{\mathrm{V}} \approx 1$ while $R_{\mathrm{VI}} \approx 2.1$ (considering the average extinction curve of Savage & Mathis 1979). For instance, we find that for $b_{\mathrm{V}} = b_{\mathrm{I}} = 0.2, A_{\mathrm{V}} = 2.1$ and $A_{\mathrm{I}} = 1.0, R'_{\mathrm{VI}} = 1.5$ for $f = 0.23$ (assuming $A_{0,\mathrm{V\ or\ I}} = 0$). Thus, observations in two well separated bands can be used to get some information on cloud structure, even in the degenerate case where $\log(N_{\mathrm{r}}) = a + bm$ for which no constraint can be drawn from the magnitude distribution alone. For a more general $N_{\mathrm{r}}(m)$, this remains true although it may be more difficult to extract this information. Another difficulty is that the expected $R_{\mathrm{VI}}$ value is not known a priori since it varies from place to place (Cardelli et al. 1989). Nevertheless, the wavelength dependence of the apparent extinction at least provides a prediction which may be used as an additional check: if the cloud studied is close to uniform, then $A'$ should vary with wavelength in a way that is consistent with the anticipated range of extinction laws. Interestingly, this test is – as the one discussed in Sect. 2.2.1 – equally sensitive to fluctuations at all scales below the field size. To our knowledge, such a test has not been made previously (see however Dickman & Herbst 1990, who determined magnitude distributions at several wavelengths). Since star counts are quite tedious when not performed in an automatic way, they are generally made at one band only and are then reduced to the V band assuming a standard extinction law.

We now show that results on cloud structure can be obtained efficiently by considering together measurements performed in two distinct bands.

### *2.4. Two-band distributions*

In the previous sections, counts in each of the bands considered (V and I for instance or any other pairs of bands) were treated separately. It is also of interest to study the full 2D distribution of stars in the plane ($m_{\mathrm{V}}$, $m_{\mathrm{I}}$). Indeed, while the 1D distributions are quite smooth, stars occupy a relatively small fraction of the accessible domain in any magnitude–magnitude diagram, a feature which will prove to be of great help to characterize the effects of the obscuring cloud (Sect. 3). In particular, star colors (e.g. V − I) are spread over a well defined and relatively limited range. When seen through a uniform cloud, stars will appear redder but to first order, the scatter of their colors will remain the same. On the contrary, this quantity will be significantly increased for a clumpy cloud due to the dispersion of reddenings.

As in Sect. 2.2, the magnitude distribution for stars seen through the cloud and with magnitudes less than $m_{\mathrm{V}}$ in V and $m_{\mathrm{I}}$ in I, $N_{\mathrm{c}}(m_{\mathrm{V}}, m_{\mathrm{I}})$, can be related to $N_{\mathrm{r}}(m_{\mathrm{V}}, m_{\mathrm{I}})$ through:

$$N_{\mathrm{c}}(m_{\mathrm{V}}, m_{\mathrm{I}}) = \int_0^\infty \int_0^\infty p(A_{\mathrm{V}}, A_{\mathrm{I}}) N_{\mathrm{r}}(m_{\mathrm{V}} - A_{\mathrm{V}}, m_{\mathrm{I}} - A_{\mathrm{I}}) dA_{\mathrm{V}} dA_{\mathrm{I}}$$

The above relation involves the 2D distribution of $(A_{\mathrm{V}}, A_{\mathrm{I}})$ values, $p(A_{\mathrm{V}}, A_{\mathrm{I}})$, which in principle allows to include variations of the ratio $A_{\mathrm{V}}/A_{\mathrm{I}}$ (i.e. fluctuations of grain properties). $N_{\mathrm{c}}(m_{\mathrm{V}}, m_{\mathrm{I}})$ contains much more information than the two separate 1D distributions and can be used more efficiently to investigate the fluctuations of the extinction. However, the accurate determination of $N_{\mathrm{c}}(m_{\mathrm{V}}, m_{\mathrm{I}})$ would require the measurement of V and I magnitudes for a very large number of stars. In practice, it will be convenient to build the projection of $N_{\mathrm{c}}$ on some selected axis and for instance consider the distribution of V − I colors. This point will be treated in more details in the next section where we present the optical data obtained for a low latitude cloud.

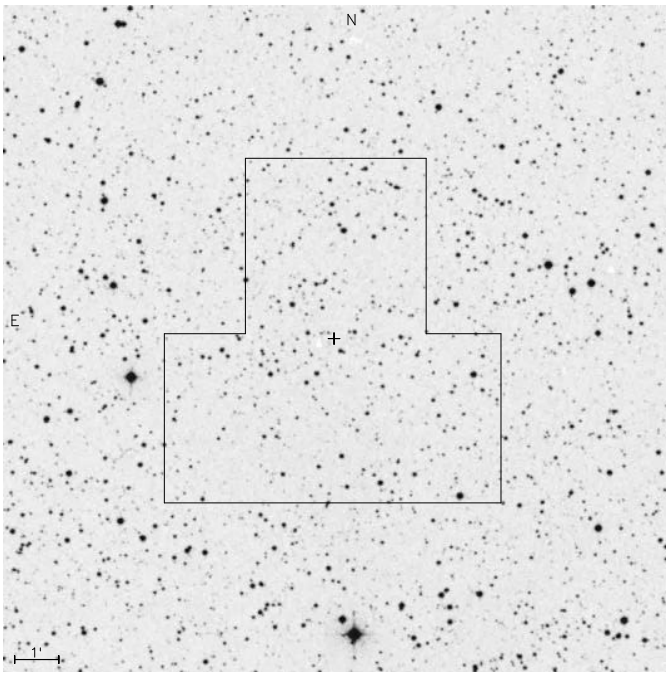


**Fig. 2.** Finding chart for the cloud field (from POSS O plates)

## 3. Photometric observations of a low latitude cloud and implications

### *3.1. Selection of the cloud*

The methods discussed above are based on the determination of magnitude distributions which requires the detection of a large number of stars (typically more than one thousand). Further, to isolate the effect of small scale variations of $A$, the field selected should be free of strong extinction gradients, which severely limits its extent. These conditions altogether imply the selection of a low galactic latitude region. In order to avoid possible confusion problems (with several distinct clouds along the line of sight, which would render the interpretation much more difficult), clouds at $l > 90°$ have to be considered. We also wish the selected cloud to be as closeby as possible, in order i) to avoid any significant contamination by stars located in front it and ii) to achieve a good linear resolution. This condition is reached by choosing clouds some parts of which appear completely free of any star on the POSS prints. Of course, it is not these regions which we select but rather translucent areas where

**Table 1.** Journal of imaging observations

| Date – Site | Field | Filter | Integration time | Comments |
|---|---|---|---|---|
| 15.11.93 – OPM[a] | CF/1 | B | 600&1800 s | |
| ” | /2 | | 1800 s | Seeing: $\sim 2''$ |
| 16.11.93 – OPM | /3 | | 1800 s | |
| ” | /4 | | 120 s | Intercalibration field |
| 17.11.93 – OPM | CF/1 | V | 900 s | |
| ” | /2 | | 720 s | Seeing: $\sim 1.5''$ |
| ” | /3 | | 720 s | No intercalibration field[b] but large overlap between CF/1, 2 and 3 |
| 15.11.93 – OPM | CF/1 | r | 300&420 s | |
| ” | /2 | | 600 s | Seeing $\sim 2''$ |
| 16.11.93 – OPM | /3 | | 600 s | |
| ” | /4 | | 138 s | Intercalibration field |
| 17.11.93 – OPM | CF/1 | i | 600 s | Calibration with N7790 |
| ” | /2 | | 480 s | Seeing $\sim 1.5''$ |
| ” | /3 | | 480 s | No intercalibration field[b] but large overlap between CF/1, 2 and 3 |
| 14.12.93 – OHP[c] | RF/1 | B | 900 s | |
| ” | /2 | | 900 s | Seeing: $\sim 3''$ |
| ” | /3 | | 90 s | Intercalibration field |
| 14.12.93 – OHP | RF/1 | V | 560 s | ” |
| ” | /2 | | 560 s | |
| ” | /3 | | 60 s | ” |
| 14.12.93 – OHP | RF/1 | $R_C$ | 420 s | ” |
| ” | /2 | | 420 s | |
| ” | /3 | | 60 s | |
| 14.12.93 – OHP | RF/1 | i | 300 s | ” |
| ” | /2 | | 300 s | |
| ” | /3 | | 60 s | |

[a] Observatoire du Pic de Midi.
[b] The intercalibration frames CF/4 and RF/3 have been reobserved at OHP in nov. 1994 to check the relative calibrations.
[c] Observatoire de Haute-Provence.

the number density of stars is typically reduced by a factor of a few as compared to the nearby regions with the highest density.

We selected a field (CF in the following) over which stars appear to be spread rather uniformly (absence of strong gradients for $A_V$), centered near the position $l = 92.6°$ and $b = -4.33°$ (see Fig. 2) and covering an area of 45 arcmin$^2$. It is located at the western end of the large complex associated with the open cluster IC5146. This cloud has been studied extensively in the $^{12}$CO and $^{13}$CO lines by Dobashi et al. (1992). Using near infrared photometry, Lada et al. (1994) have recently performed a detailed study of the extinction over a large fraction of this complex (we were not aware of this work when our study was undertaken and unfortunately, the cloud field selected happens to lie outside the region surveyed in the infrared). A reference field (RF in the following) was selected on the blue POSS prints, within “windows” which display the highest number density of stars (field center: $l = 90.6°$, $b = -3.8°$; area: 73 arcmin$^2$). These regions appear well uniform over a relatively large extent and should suffer from only a moderate diffuse extinction. In the following, we assume for simplicity that the extinction is zero in RF; in fact, our analysis is sensitive only to the difference between the diffuse extinction in CF and RF, which we believe to be very small as discussed in more detail in Sect. 6.1. CF and RF fields are located at nearly the same latitude and separated by only 2 degrees in longitude so that the stellar population in RF should be a very good estimate of that in CF if the obscuring cloud were absent.

### *3.2. Optical photometric observations*

Observations have been performed using both the 1.20 m telescope at Observatoire de Haute-Provence (OHP) and the 2 m telescope at the Observatoire du Pic du Midi (OPM). The journal of observations is given in Table 1. The filters used at both sites are similar, but in the R band (R Cousins at OHP and r Gunn at OPM). Measurements made through the r filter at OPM have been transformed in the Cousins system; these corrections remain quite small for most stars (a few 0.01 mag.). Field CF consists in a mosaic of 3 adjacents CCD images (stars common to each pair of frames allowed an accurate intercalibration of these images). Standard stars were used for calibrations but the weather conditions were generally not very good and the resulting accuracy is probably not better than a few 0.1 mag. However, special care was paid to get a good relative calibration between

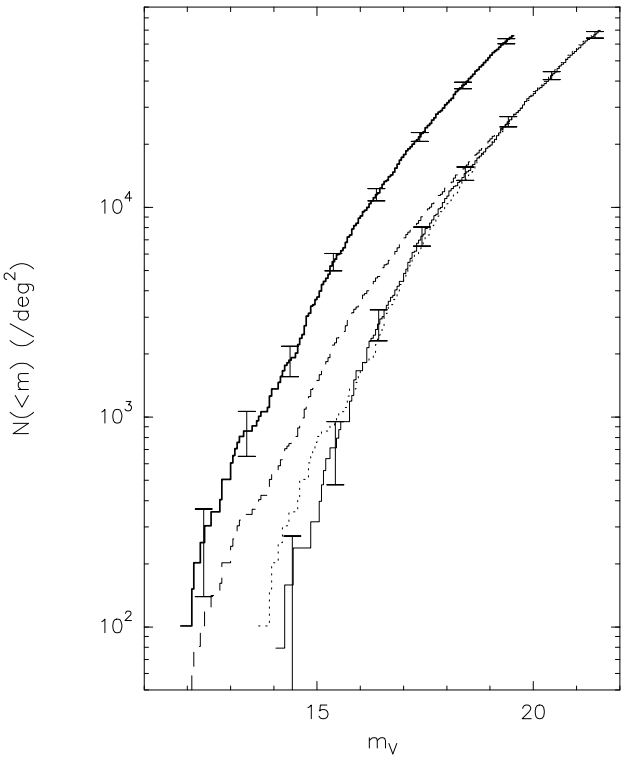


**Fig. 3.** The cumulative magnitude distribution in the V band for the reference (heavy line) and cloud field (thin line). Also shown are the distributions expected from a uniform slab (with extinction 1.8; dotted line) and a clumpy cloud (with surface covering factor $f = 0.6$, chosen so as to match the counts at $m_V \approx 19.5$; dashed line). Statistical uncertainties are shown (1 $\sigma$ error bars)

the cloud and reference fields. To achieve this, we successively obtained short integration time images ($\Delta t \approx$ a few minutes) of CF and RF; we are confident that the error in the intercalibration is no larger than 0.1 mag.

### *3.3. Reduction of the data*

All CCD images have been treated in the classical way (bias subtraction and flat field correction) using the ESO software package MIDAS. Next, our main objective is to build the magnitude distribution for all fields and filters considered. To this aim, we have used the Inventory Context of MIDAS developed by A. Kruszewsky. This set of procedures allows to perform in an automatic way the detection, measurement of position and magnitude of objects on photometric fields. For our magnitude limits, the number of galaxies expected in our fields is quite small and it was therefore not necessary to perform the classification step (the seeing achieved would anyway not have been good enough to do this efficiently). For the analysis, one important parameter to determine for each filter X is the magnitude $m_{\mathrm{lim,X}}$ up to which the distribution is complete. The latter is likely to be somewhat brighter than the detection limit because the fields are relatively crowded (especially RF) and the automatic procedure may be only partially efficient in finding the faintest detectable objects when located close to brighter ones. A good estimate for $m_{\mathrm{lim}}$ can be obtained by examining the shape of the observed differential distribution, $N'(m)$, since the latter is expected to be smooth and featureless. To get an independent estimate, we also generated simulated stellar fields with properties (seeing, noise, number density and magnitude distribution of stars) similar to that of CF and RF and treated them exactly in the same way as our data: the comparison between the assumed and measured magnitude distributions then directly provides $m_{\mathrm{lim}}$. Both estimates were found to be comparable with limiting magnitudes in the B, V, R and i bands of 21.0, 21.5, 20.5, 20.5 for the CF field and 20.0, 19.5, 19.0, 18.5 for the RF field respectively. The detection limit is about one magnitude fainter. The accuracy of the magnitude estimates is better than 0.1 mag for the faintest objects included and smaller for brighter stars.

### *3.4. Statistical analysis and results*

#### 3.4.1. Single band measurements

The cumulative distributions $N_{\mathrm{c}}$ and $N_{\mathrm{r}}$ are shown for the V band and fields CF and RF in Fig. 3. A first remark is that both distributions do show significant curvature (i.e. departure from an exponential law). The same is true in other bands. As discussed above, it is then possible to derive some constraints on the structure of the cloud.

To judge whether or not a given model (i.e. $p(A)$) provides an acceptable fit, we have adopted the following procedure. Stars from the reference field are used to generate a "simulated" obscured field associated with the cloud model considered. This field has the same size as the cloud field and include a sample of stars which is complete up to a magnitude $m_{\mathrm{lim,r}} + A_{\mathrm{min}}$ where $A_{\mathrm{min}}$ is the minimum value of $A$ in CF for which $p(A) \neq 0$ and $m_{\mathrm{lim,r}}$ the completeness magnitude for RF (recall that we assume $A = 0$ in RF). Next, we compare these data to those involving the cloud field (complete up to $m_{\mathrm{lim,c}}$). The range over which the two sets of data can be compared is defined by $m < m_{\mathrm{lim}}$ where

$$m_{\mathrm{lim}} = \min(m_{\mathrm{lim,r}} + A_{\mathrm{min}}; m_{\mathrm{lim,c}}) \ .$$

We first check that the shape of the cloud and model distributions, $N_{\mathrm{c}}(m)$ and $N_{\mathrm{m}}(m)$, are compatible. To this purpose, we use the Kolmogorov-Smirnov test statistics (a significance level of 95% is adopted throughout). The latter involves the maximum difference $D$ between the normalized distributions ($N_{\mathrm{c}}(m)/N_{\mathrm{c}}(m_{\mathrm{lim}})$ and $N_{\mathrm{m}}(m)/N_{\mathrm{m}}(m_{\mathrm{lim}})$). Since both distributions are known with finite accuracy, the parameter to be considered is $Z = (N)^{1/2}D$ (Peacock 1983), where $N$ is given by

$$N = \sqrt{\frac{N_{\mathrm{m}}(m_{\mathrm{lim}}N_{\mathrm{c}}(m_{\mathrm{lim}})}{N_{\mathrm{m}}(m_{\mathrm{lim}} + N_{\mathrm{c}}(m_{\mathrm{lim}})}} \ .$$

$R_{\mathrm{Z}}$ is then defined as the ratio of Z and the critical value corresponding to $N$ and to the confidence level adopted (if $R_{\mathrm{Z}} > 1$, the model can be rejected at the 95% confidence level). We further need to verify that the total number of stars $N_{\mathrm{c}}(m_{\mathrm{lim}})$

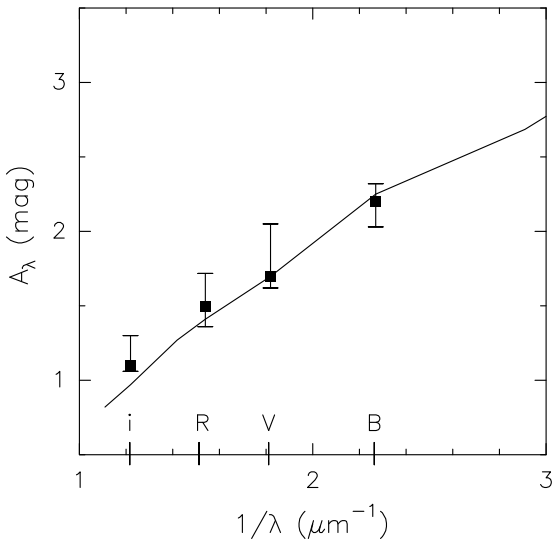


**Fig. 4.** The extinction derived in the B, V, R and i bands for homogeneous models (filled squares). Shown for comparison is the average extinction curve (line) as given by Savage & Mathis (1979) for $A_V = 1.7$ mag

and $N_m(m_{lim})$ are compatible (the K-S test apply to normalized distributions only). To this aim, we define $R_N$ as

$$R_N = \frac{N_m(m_{lim}) - N_c(m_{lim})}{\sigma(N_m(m_{lim}) - N_c(m_{lim}))}$$

where $\sigma(N_c(m_{lim}) - N_m(m_{lim}))$, the rms error on $N_c(m_{lim}) - N_m(m_{lim})$, can be computed easily. Numbers are considered to be compatible when $|R_N|$ is less than 2 (this roughly corresponds to a significance level of 95%).

Let us first qualitatively compare the observed distribution to those expected from the two extreme models H and C (the latter are displayed as well in Fig. 3). The computed "model distribution", $N_m$, is derived from relation (4), with either $f = 0$ for model H or $A_0 = 0$ for model C, $A_0$ and $f$ being chosen such that computed and observed integrated counts are equal ($N_m(m_{lim}) = N_c(m_{lim})$). It is immediately clear that model H gives a much better fit to the data. This remarkably simple result can be further considered as a strong test regarding the overall consistency of our data set and reduction procedures; indeed any error or bias in the analysis would a priori render a good fit difficult (or impossible) to obtain (note that for a given $N_r$, not all $N_c$ are acceptable).

The objective test procedure described above confirms that for all B, V, R and i bands, a cloud exclusively made of opaque clumps (model C) can be rejected whereas an homogeneous cloud provides an acceptable fit. It is then possible to infer values for $A_0(B), \ldots A_0(i)$. The latter are plotted in Fig. 4 with uncertainties obtained by allowing $R_N$ to vary as far as $|R_N| < 1$. The $A_0(\lambda)$ thus obtained closely follows the average extinction law given by Savage and Mathis (1979) and is clearly compatible with the range observed for extinction curves in the galaxy. As discussed in Sect. 2.3, this result is an additional indication that the cloud does not show strong departures from uniformity.

From single band data, we could discriminate between the two extreme models H and C. However, it can be anticipated easily that several more or less homogeneous models will remain acceptable as well. In order to assess how clumpy are the models which are just marginally acceptable, let us consider the two-parameter model CH which allows a continuous transition from H to C. Starting from H, one can gradually increase $f$ while reducing the extinction of the interclump phase so as to impose $N_m(m_{lim}) \approx N_c(m_{lim})$. Thus, for the V band, only models with $f$ larger than 0.20 (which correspond to $A_0(V) < 1.50$) can be excluded. We also considered models with two discrete values for $A$, $A_1$ and $A_2$(we note $p_1 = p(A_1)$ and $p_2 = p(A_2)$). To quantify how much the model cloud departs from a uniform one regarding the transfer of radiation, we compute the ratio of the effective to the average extinction, $A_{eff}/\langle A\rangle$ (this is not possible with model CH since $\langle A\rangle$ is infinite). This ratio may be expressed as

$$\frac{A_{eff}}{\langle A\rangle}(V) = \frac{-2.5\log(p_1 10^{-\frac{A_1(V)}{2.5}} + p_2 10^{-\frac{A_2(V)}{2.5}})}{p_1 A_1(V) + p_2 A_2(V)} .$$

In particular, it is important to estimate its value at UV wavelengths where photons play an important role in the chemistry. We choose a representative value of 1500 Å for which $A_{1\text{ or }2}(UV) = 2.6 A_{1\text{ or }2}(V)$ and get $A'/\langle A\rangle(UV)$ by substituting $A_{1\text{ or }2}(UV)$ to $A_{1\text{ or }2}(V)$ in the above formula. We have adopted here the average extinction curve of Savage & Mathis (1979); for a law associated with a larger $A(V)/E(B-V)$ ratio, the $A(UV)/A(V)$ value will be smaller (Cardelli et al. 1989). Fragmentation will have significant effects on the transfer when the ratio is notably smaller than unity ($A_{eff}/\langle A\rangle = 1$ for uniform clouds). By varying $A_1$, $A_2$ and $p_1$ ($p_2 = 1 - p_1$) inside reasonable ranges, we find the smallest acceptable values of $A_{eff}/\langle A\rangle$ (UV) to be around 0.4.

Hence, we conclude that a relatively broad range of models cannot be rejected. The fact that single band distributions only provide loose constraints on $p(A)$ can be understood easily. Indeed, if the differential distribution $N_c'$ displayed a marked feature (a break or a narrow bump ...), this would help considerably to select the appropriate models (for instance, one would see more clearly if the curve for $N_c$ is shifted rather horizontally or vertically). While single-band distributions are quite smooth, 2-band distributions display sharp features which will help to narrow down the range of acceptable models.

### 3.4.2. Two-band measurements

From observations in two different bands, it is easy to build a sample of stars detected at both wavelengths, using positional agreement criteria. One can anticipate that the use of two well separated bands will be more fruitful because of a larger difference in extinction. Moreover, we detect far less stars at B than in other bands. For these two reasons, the choice of V and i bands appears as the best compromise. The corresponding data are shown in a $m_V - m_I$ plot (Fig. 5) for both CF and RF. It is immediately clear that the cloud obscuring CF does not enhance the scatter very much.

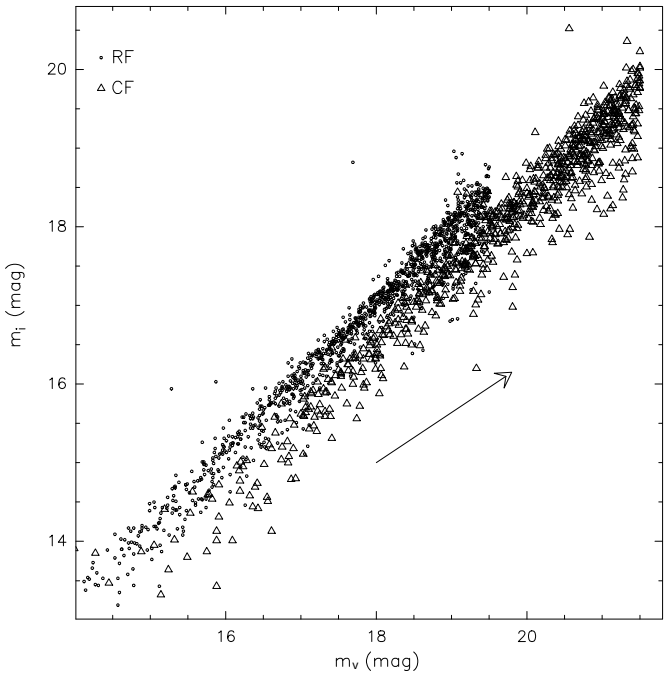


**Fig. 5.** Plot of the i versus V magnitude for stars in the reference field (RF, dots) and cloud field (CF, empty triangles). A reddening vector corresponding to $A_V = 1.9$ and $A_I/A_V = 0.64$ is shown

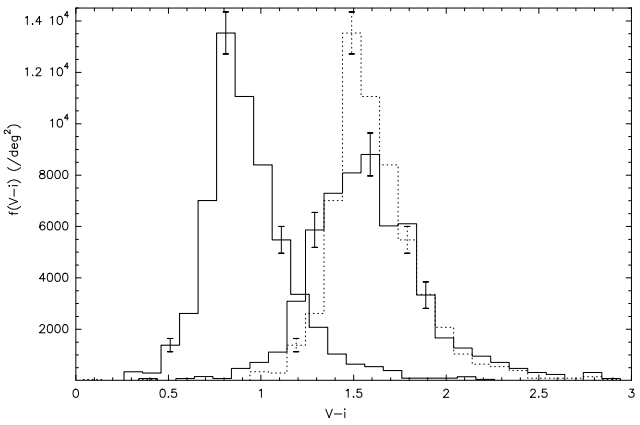


**Fig. 6.** Normalized distributions of the V − i colors for stars in the reference field (thick line) and in the cloud field (thin line). For comparison, we show the distribution expected from a homogeneous models with $E(V - i) = 0.68$. One $\sigma$ uncertainties are indicated

We first attempted to apply a procedure similar to that described above to decide which cloud models are acceptable. The 2D version of the Kolmogorov- Smirnov test as developped by Peacok (1983) and Fasano & Franceschini (1987) and applied to variables $m_V$ and $m_I$ was used to this purpose but turned out to provide no tighter constraints as compared to those derived from one- band samples. This is because such an analysis does not take advantage of the fact that, intrinsically (i.e. in RF), stars are distributed over a narrow strip in Fig. 5. Since we wish to measure the additional dispersion induced by the cloud in the ($m_V$, $m_I$) plane, it is appropriate to consider a variable $x$ such that the spread of $x$ for RF stars, $\Delta x$(RF), is minimum. This is achieved by choosing $m_V - m_I$ and $m_V$ as new variables. While $m_V$ and $m_I$ were strongly correlated through the distance, $m_V - m_I$ and $m_V$ are nearly uncorrelated ($m_V - m_I$ being mainly related to the spectral type and $m_V$ to the distance). In fact, there is a weak tendency for fainter stars to be slightly redder, an effect which could be due to either to the presence of diffuse extinction or to an intrinsic evolution of the stellar population with distance. Then, $m_V - km_I$ (where $k$ is the slope of the ($m_V$, $m_I$) correlation) would even be a better choice; however, since $k$ is quite close to 1 ($k \approx 1.07$ for V and i), we just considered the usual $m_V - m_I$ colors.

The test procedure described in Sect. 3.4.1 has been adapted. First, we define the 2D range over which the model (computed) and observed distributions can be compared (this is given by $m_{lim}$(V) and $m_{lim}$(i)). The distribution for $m_V - m_I$ is computed for stars located in this domain. We then check the agreement between the total number of stars ($|R_N| \leq 2$) and the shape of the $m_V - m_I$ and $m_V$ distributions. For this latter task, we used the 1D K-S test applied to each variable (the 2D version of the test was found to give the same results, as expected since both quantities are nearly independent).

In Fig. 6, we show the distributions for $m_V - m_I$ observed in CF and RF together with that expected from a uniform cloud with $E(V - i) = 0.68$ mag. The presence of the cloud results, to first order, in a shift of the histogram. Moreover, one can notice that the CF distribution is somewhat broader than the computed one, due to fluctuations of $E(V - i)$ (note than the CF distribution could in no way have been narrower than the RF one!). Indeed, all uniform models are ruled out by the test procedure, the K-S test on the shape of the $m_V - m_I$ histogram being by far the most restrictive (at best, one gets $R_Z \approx 1.4$ for the latter). In this search, the ratio $A_i/A_V$ was allowed to vary around the value 0.6 determined earlier. A similar result is obtained when considering the independent (B,R) data.

For C models, the normalized V − i distribution ($f(V - i)$) is similar to that for RF, stars being removed regardless of their color while for CH clouds, $f(V - i)$ is given by the distribution expected from a uniform cloud (with extinction $A_0$(CH)). Therefore, these classes of models can be excluded too. An estimate of the range covered by $E(V - i)$ (hereafter $E$) values can be obtained directly from inspection of Fig. 6. Indeed, since $E$ is uncorrelated to the V − i color of background stars, the range expected for V − i in CF is $[(V - i)_{min} + E_{min}, (V - i)_{max} + E_{max}]$ where $[(V - i)_{min}, (V - i)_{max}]$ is the range of (V − i) values in RF and $[E_{min}, E_{max}]$ that of $E$ values in CF (the distribution of (V − i) in RF, CF and $p(E)$ are in fact approximately related by a convolution equation; this is however not an exact relation because the effect of limiting magnitudes is more complex than in Eqn (2) and can be taken into account only through the procedure described above). We thus conclude that the interval covered by $E(V - i)$, [0.4, 1.2], is quite limited. In particular, there are no pronounced holes ($E < 0.4$) nor regions with reddenings in the range $1.2 < E < 2.0$ (we come back later on constraints that can be obtained on completely opaque frag-

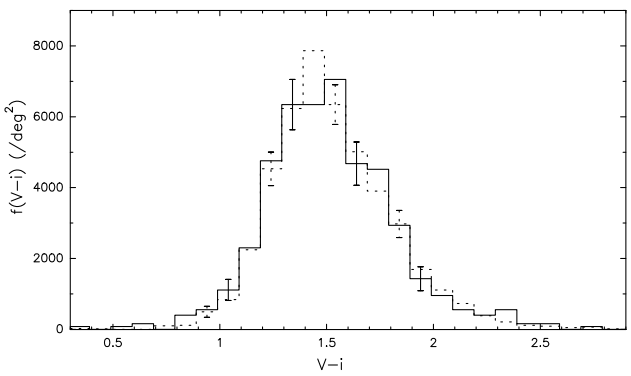


**Fig. 7.** Normalized distribution of the V − i colors for stars observed in the cloud field (full line). The distribution computed from a model with 3 discrete values for $E(\mathrm{V}-\mathrm{i})$ which is accepted by the test procedure (see text)

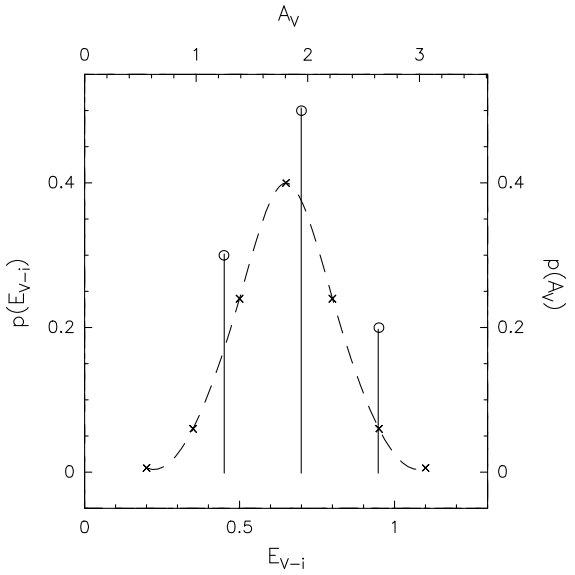


**Fig. 8.** Distribution functions of $E(\mathrm{V}-\mathrm{i})$ or $A_\mathrm{V}$ that give a good fit to the observed colors and magnitudes in CF (circles: best 3-value distribution; crosses: best gaussian fit)

ments). Since we have information for more than one thousand lines of sight through the cloud, we could have missed (small) regions of low ($E < 0.4$) or high ($1.2 < E < 2.0$) opacities only if their surface covering factor is smaller than $f \approx 0.01$.

We now attempt to find a model which allows to fit the observed distributions. An additional complication when dealing with two-band data is that the ratio $A_\mathrm{I}/A_\mathrm{V}$ could vary across the field (this is not unrealistic given the large local variations observed for some types of grains; Boulanger et al. 1990). Our data being not well adapted to address this question, we shall assume a uniform value in the range [0.5, 0.7]. The test on $f(\mathrm{V}-\mathrm{i})$ being the most constraining, it is more convenient to determine first the distribution for $E(\mathrm{V}-\mathrm{i})$ (hereafter $E$). For simplicity, we represent $p(E)$ by using a few discrete values and adopt the form

$$p(E) = \sum_{j=1}^{j=n} p_j \delta(E - E_j) \quad \text{with} \quad \sum_{j=1}^{j=n} p_j = 1 \ .$$

A given set of $(p_j, E_j)$ and a value for $A_\mathrm{i}/A_\mathrm{V}$ entirely define the model (in the sense that it allows to compute $N_\mathrm{m}$ from $N_\mathrm{r}$; however, as discussed above, the exact associated 3D distribution of the dust is obviously not completely defined by these parameters).

We first tried $n = 2$ but no acceptable fit could be obtained: when $E_2 - E_1$ is large enough to account for the width of $f_\mathrm{c}(\mathrm{V}-\mathrm{i})$, the distribution appears markedly bimodal contrary to what is observed. At least three values are required. To get a first solution, we select realistic values for $E_1$, $E_2$ and $E_3$ and then write for $E$ an equation similar to (2) which, in our case, can be put in the form of a linear system in $p_1$, $p_2$ and $p_3$. Next, a better solution can be obtained by allowing small variations of the $p_j$ and $E_j$. Thus a model with $p_{1,2,3} = 0.30, 0.50, 0.20$, $E_{1,2,3} = 0.45, 0.70, 0.95$ and $A_\mathrm{I}/A_\mathrm{V} = 0.64$ gives quite a good fit with $R_\mathrm{Z} = 0.38, 0.45, 0.46$ for the 1D K-S test on the V − i, V and i distributions respectively and $R_\mathrm{N} = -0.2$ (see Fig. 7). The corresponding values are 1.29, 2.00, 2.71 for $A_\mathrm{V}$ ($\langle A_\mathrm{V}\rangle = 1.93$ and $\sigma(A_\mathrm{V}) = 0.49$) and 0.84, 1.30, 1.76 for $A_\mathrm{I}$. Only slight deviations from the above solution are allowed for the $E_j$ and $p_j$. On the other hand, the $A_\mathrm{I}/A_\mathrm{V}$ ratio is not accurately determined, the acceptable range being [0.58–0.68].

To verify that the obtained $p(E)$ or $p(A_\mathrm{V})$ is not too much dependent on the a priori adopted form, we also tried a gaussian distribution (discretized on 7 values for convenience). The result is illustrated in Fig. 8 where we plot both the gaussian and the 3-valued best solutions. We note that the average as well as the variance are quite similar in these two cases (relative variations less than 5%). We are therefore confident that the above solutions truly represent the main features of the distribution of the extinction across the field. Strong additional support to this conclusion is provided by the completely independent (B,R) samples. Indeed, we repeated the analysis for these bands and found that the best solutions can be directly inferred from those which fit the (V, i) data if $A_\mathrm{R}/A_\mathrm{B} = 0.69$ and $E(\mathrm{B}-\mathrm{R}) \approx E(\mathrm{V}-\mathrm{i})$.

Interestingly, we find that for the optimal solution quoted above, the ratio $A_\mathrm{eff}/\langle A\rangle(\mathrm{UV})$ is 0.85. Among all acceptable solutions, this ratio is never smaller than 0.75. As noted above, these results somewhat depend on the assumed extinction curve; however, a total to selective extinction ratio $(A(\mathrm{V})/E(\mathrm{B}-\mathrm{V}))$ larger than 3.1 (which might be expected for molecular material), would imply that the values quoted above are even closer to unity. A safe conclusion is therefore that small scale fluctuations of the opacity are present, but their amplitude is too small to notably affect the transfer of continuum UV radiation.

As quoted earlier, our method could be biased against totally opaque regions since no star can be seen through the latter. It is therefore important to examine which constraint can be put on the fraction of the surface that they may cover. To this purpose, we start from the best three-value solution obtained above and consider in addition to the $E_1$, $E_2$, $E_3$ color excesses, a fourth arbitrarily large value $E_4$, (with $p(E = E_4) = p_4$) such

that stars suffering a reddening $E_4$ are so faint that none is detected. Next, we gradually increase $p_4$ ($p_1/p_2$ and $p_1/p_3$ being kept constant) up to a critical value for which the fit is no longer acceptable. We find a critical value $p_4 = 0.05$ set by the condition $R_N = -2$. Thus, only a small fraction of the cloud could be masked by completely opaque material. Even this possibility appears quite unlikely because in any realistic model, one should observe in the (V,i) plot a continuous distribution extending up to the limiting magnitude in the V band. On the contrary, it is clear in Fig. 5 that the strip of points associated with CF stars is definitely bounded on its red side. Then, although it is, strictly speaking, not possible to estimate the average extinction with this method, we are quite confident here that the above 3-value (or Gaussian) solution fully describes the distribution of extinction values across the cloud field. Note that the method constrains more directly the absence of "holes" in the cloud (these would leave a fraction of unreddened stars which would be very easy to notice in Figs. 5 and 6).

### *3.5. Mapping of the extinction below the arcmin scale*

As already mentioned, the method described above is similarly sensitive to variations at all scales down to a few $\mu$arcsec. Then, it does not give any information about the scale of the extinction fluctuations nor about their spatial distribution. We can however determine easily the contribution of large scales by examining the number and properties of stars as a function of position in the field. Classical star counts could be used but, since we have multi-band data, we can get much more accurate results (or for a given accuracy much better angular resolution) by considering the color of stars inside small CF cells (such a method has already been used by Witt et al. 1990 and, in the near infrared by Lada et al. 1994). We make the assumption that within any CF cell, the extinction (or reddening) can be considered uniform (we shall examine next whether the data are consistent with this hypothesis). Then, the reddening can be directly inferred from the difference between the average V − i color for stars in the CF cell and in RF.

In order to estimate the accuracy of such a determination, we performed Monte-Carlo simulations. We select $N^*$ values for V − i drawn from a probability distribution given by the RF data and compute the average and median over these $N^*$ stars. This procedure is repeated one thousand times to estimate the accuracy with which the median and average are returned. The uncertainty is found to be slightly smaller for the median; an additional reason to prefer this estimator is that it is more robust and less affected if a few outliers are present (due to particle impacts on some stellar images for instance). For $N^* = 5, 10, 20$ we get a 1 $\sigma$ uncertainty on $E(V-i)$ of 0.09, 0.06 and 0.04 mag. respectively or 0.25, 0.17 and 0.11 on $A_V$ (with $A_i = 0.64\,A_V$).

To cover the whole cloud field, it was convenient to choose a cell size of 42" which results in about 10 stars per cell (note that, strictly speaking, the accuracy in the determination of $A_V$ is not uniform because the actual number of stars varies from one cell to another due to i) Poissonian fluctuations and ii) systematic variations of $A_V$; an alternative procedure would consist in adjusting each cell so as to include a fixed number of stars but the angular resolution would then not be well determined). We checked that the local median (V − i) color is well uniform throughout RF and adopted for subtraction the median (V − i) color computed over the entire RF field, (V − i) = 0.95. A fully sampled map was generated with adjacent cell centers separated by 21" (Fig. 9). A well organized pattern is seen, indicating that at least part of the fluctuations comes from scales of about 1′ or larger. As a check, we also generated a map for $E$(B − R) (with a resolution about two times worse due to a lower number of stars); the same overall pattern is observed (we also verified that the variation of the number of stars, although much more noisy, is consistent with that pattern). Further, it turns out that the range covered by $E$(V − i) in cells well corresponds to the $p(E)$ previously obtained which suggests that the large scale variations may account for a large fraction of the whole fluctuations. To determine to which extent this is true, we use the $E$(V − i)

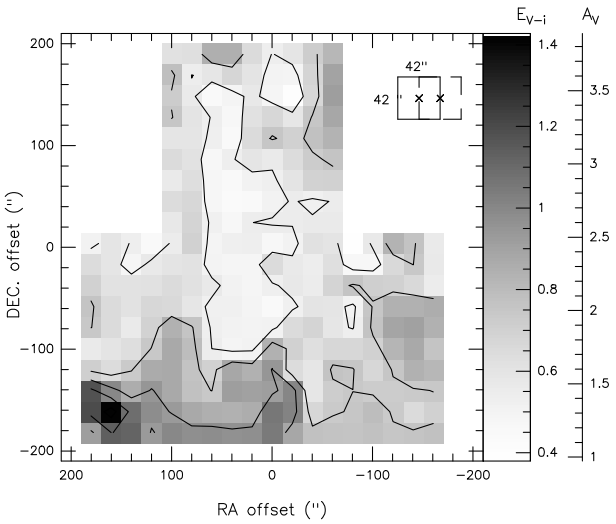


**Fig. 9.** Map for $E$(V − i) in the cloud field derived from the median of V − i colors in 42 × 42″ cells. The contour levels for $E$(V − i) are 0.55, 0.75, 0.95 and 1.15 mag

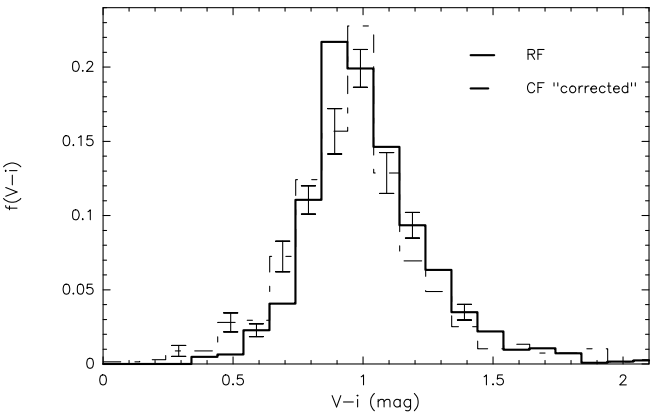


**Fig. 10.** Distribution of corrected V − i colors (dashed line) compared to the reference distribution. Values shown in Fig. 9 have been used to deredden the cloud field stars

measured in cells to deredden all stars in the cloud field, build the distribution of corrected V − i colors and compare it to the RF distribution. As can be seen in Fig. 10, both are compatible. The data thus appear consistent with our initial assumption that most of the fluctuations occur at scales larger than 42″.

### *3.6. Biases in the color excess method*

The results shown above as well as those published by Lada et al. (1994) illustrate the power of the color excess method. For the cloud of interest in our study, we could verify that structure within the cells considered have not biased the extinction estimates. However, in other conditions, significant variations may be present inside the sampling element if for instance, in an extensive survey, some cells fall just on the edge of high extinction areas (one way to check this is to compare the rms scatter of colors for stars within the cells to the intrinsic scatter; cf. Lada et al. 1994). It is therefore important to estimate how much the measurements could be affected by small scale structure. The bias is due to the fact that stars with larger reddenings suffer from a larger extinction and will be underrepresented, leading to an underestimate of the average extinction. In the extreme case of a C type cloud, the extinguished stars are not detected and the average color will be computed only over those stars which remain unreddened because they have no clump in front of them, leading to $\langle A_V \rangle = 0$! (while the true average extinction may be arbitrarily large). For real clouds, this effect increases with the amplitude of the extinction fluctuations and can be corrected only if the intrinsic two-magnitude distribution is known and if a distribution of $E$ values within the cell is assumed.

In the absence of sub-cell structure, estimates may be biased for an additional reason if the average or median color for the background population depends on magnitude. For instance, if diffuse material is present behind the cloud studied, fainter stars would appear redder in average (the average spectral type may also depend on distance and hence on magnitude). In the latter case, stars seen in a high opacity cell are characterized by an unextincted magnitude brighter than those in a low extinction cell (for a given limiting magnitude) which will tend to lower the color excess and lead again to an underestimate of the extinction. In our study, we could check that such an effect is negligible because the color depends very weakly on magnitude (see Sect. 3.4.2).

These two biases may however play some role in another context where distant galaxies are used as background objects to determine the dust opacity in the outer parts of a nearby galaxy (Zaritsky 1994; Lequeux et al. 1995). In such a circumstance, the cell size required to detect a few background objects corresponds to a large linear distance, even for closeby galaxies. The patchy nature of extinction may then lead to significantly underestimate the true amount of dust in the latter. Further, the dependence of galaxy colors on magnitude (through the redshift) due to both the K correction and cosmological evolution may also be of importance, especially if very deep images are used (Smail et al. 1995).

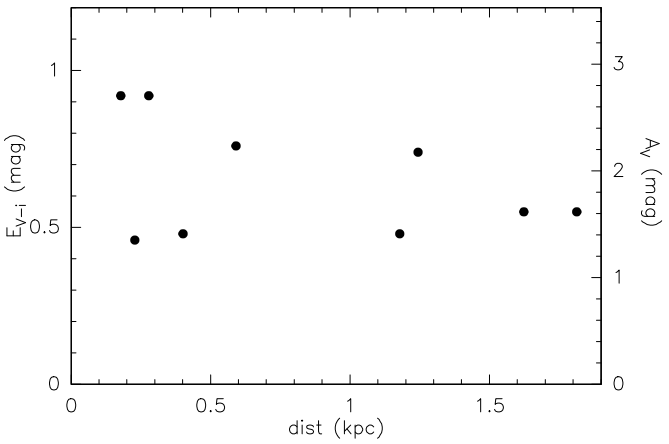


**Fig. 11.** The color excess $E(V - i)$ versus distance for the nine stars observed spectroscopically

## 4. Spectroscopic observations

Our aim was to complement the photometric data by determining the spectral type of a few stars and infer their reddening and distance. This is classically done by using Strömgren photometry of B, A and F type stars which allows to obtain accurate extinction and distance estimates and study the large scale characteristics of the extinction (Jønch-Sørensen & Knude 1994; Franco 1995). Since we also wished to investigate the small scale spatial variability of some diffuse interstellar bands (the results of this latter study will be reported in a future paper) we choosed to perform spectroscopic observations at a few Å resolution. This allows to check in an independent way the results obtained in Sect. 3 and also to constrain the distance to the cloud.

We selected 9 stars among the brightest in the cloud field. Observations were performed using the CARELEC spectrograph attached to the 1.93 m telescope at Observatoire de Haute-Provence. The spectral resolution was 8 Å and the wavelength range 3600–5600 Å. To determine spectral types, we retrieved from the CDS spectra of stars observed by Jacoby et al. (1984) and degraded them at our resolution. All stars were assumed to be from the main sequence, a reasonable assumption since in the solar neighborhood, giants represents only $\approx 2\%$ of the overall population. Since our data have not been flux calibrated, we only compared normalized spectra. The B, V, R and i magnitudes were carefully remeasured on CCD frames and stars with close neighbors for which uncertainties may be larger were discarded. Once the spectral type is obtained from CaII, HI, ... lines, we compare the V − i and B-R colors to those given by Johnson (1966) and derive $E(V - i)$ and $E(B - R)$. Using a ratio $A_I/A_V = 0.64$, we get for each of the nine stars the V band extinction, the corrected $m_V - A_V$ magnitude and finally the distance. In Fig. 11, we show the color excess $E(V - i)$ versus the distance. $E(V - i)$ (which is more accurately measured than $E(B - R)$) is observed to span the range [0.46–0.92], with an average value of about 0.6. This is well compatible with the $p(E)$ obtained in Sect. 3. The above procedure requires well cal-

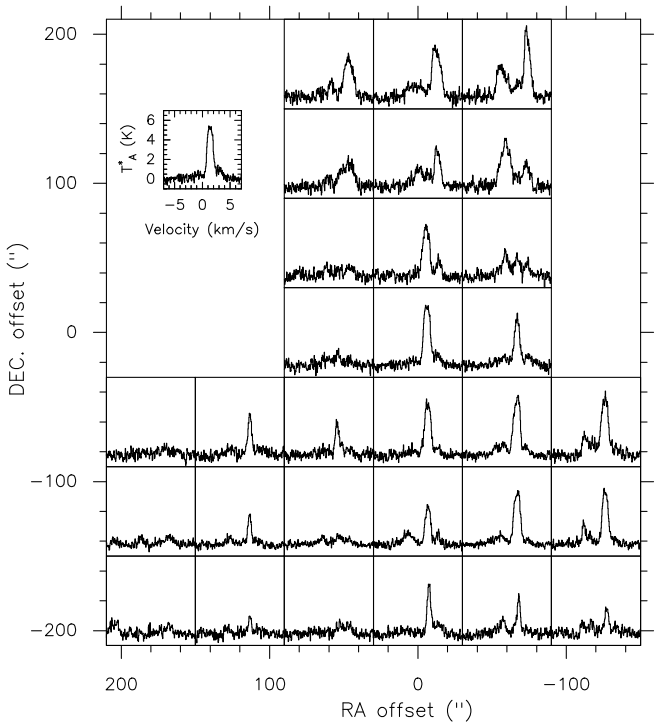


**Fig. 12.** Spectra obtained with the 30 m IRAM telescope for the $^{12}$CO($J$ = 1–0) line in the cloud field (beam: 22″). Observed positions are separated by 1 arcmin

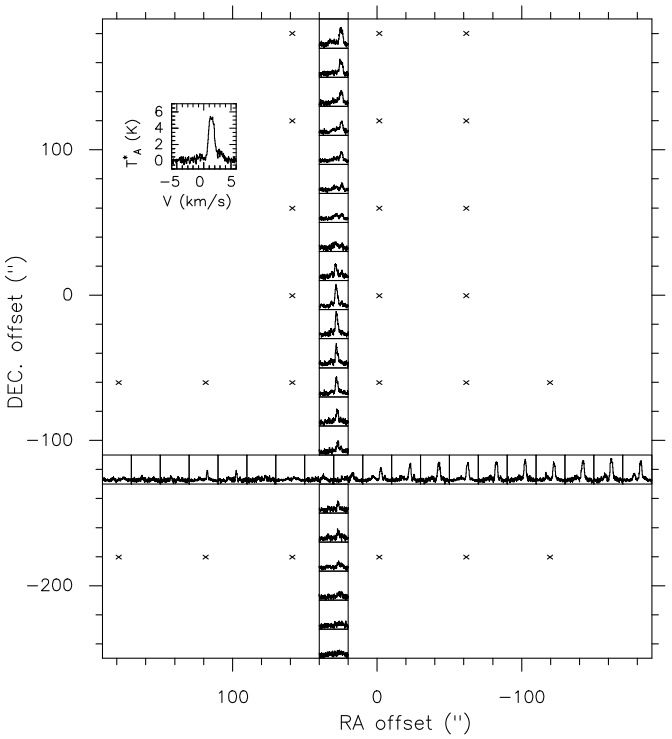


**Fig. 13.** Cuts made at RA = 30″ and DEC = −120″ for the $^{12}$CO($J$ = 1–0) spectra with a spacing of 20″. Other positions observed and displayed in Fig. 12 are shown

ibrated magnitudes and since our observations have not always been performed in good weather conditions, some additional errors may result. Indeed, although the color excess $E(B-R)$ is overall well correlated to $E(V-i)$, some scatter is observed in the relation which indicates that the final accuracy is probably not better than $\approx 0.15$ mag (the uncertainty associated with the determination of the spectral type being only about 0.05). Therefore, only the average and overall scatter of $E(V-i)$ are meaningful.

All stars appear to be significantly reddened. We then conclude that the cloud lies at $d \leq 200$ pc, the distance of the two nearest stars. This value is well smaller than the 1 kpc derived by Walker (1959) from photometric observations of the cluster IC 5146 presumably associated with the complex. Lada et al. (1994) get an estimate $d \approx 400$ pc, a value which is closer to ours. In the following, we adopt $d = 200$ pc. We also note that there is no trend for $E(V-i)$ to increase with the distance to the star (the larger value being 1.8 kpc). Therefore, extinction associated with background diffuse material should play a negligible role. We are aware that, by selecting the brightest stars, the above results may be biased towards low reddening values. Nevertheless, spectroscopic observations should at least provide estimates which fall in the range inferred from the global statistical analysis, in agreement with what we find.

## 5. High resolution CO observations

Our purpose is to compare the behaviour of extinction and $^{12}$CO emission as mass tracers. At large scales, $A_V$ is observed to scale roughly linearly with $I$(CO) for $A_V$ less than $\approx 3$ mag. (see e.g. Cernicharo & Guélin 1987). Assuming $N(H_2)$ to increase linearly with $A_V$ (Bohlin et al. 1978) this is commonly expressed in terms of the ratio $X_{CO} = N(H_2)/I(CO)$ (see Magnani & Onello 1995 for a discussion about the determination of this ratio). It is widely believed that such a relation still holds for the small regions that the millimeter wave observations allow to probe. This is however not obvious because a different behaviour may be expected at scales over which the associated extinction gets smaller than the minimum value required for efficient self-shielding. Since we could map the variations of $A_V$ with an unprecedented high spatial resolution and establish that additional fluctuations play a negligible role, we are in a good position to see whether both $H_2$ tracers behave in the same way at small scales and estimate the corresponding $X_{CO}$ ratio.

Observations were performed using the IRAM 30 m radiotelescope at Pico Veleta, Spain, in December 1994. We observed simultaneously the two transitions, $^{12}$CO($J$ = 1–0) and $^{12}$CO($J$ = 2–1). Spectra were obtained under good winter atmospheric conditions with a typical system temperature of 300 K for the 1 mm receiver and 400 K for the 3 mm receiver. The spectra were acquired by position switching with a reference ("off") position at $(+12', -1°)$; the latter does not coincide with RF (which would have been too far away) but this has no effect on

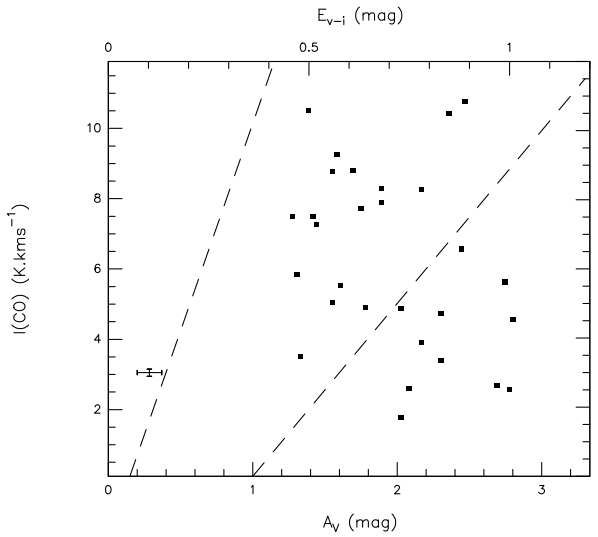


**Fig. 14.** The integrated $^{12}$CO($J$ = 1–0) line intensity, $I$(CO), versus the reddening, $E$(V − i). The area containing the data obtained at the 5 arcmin scale by Cernicharo & Guélin (1987) is comprised between the two dashed lines

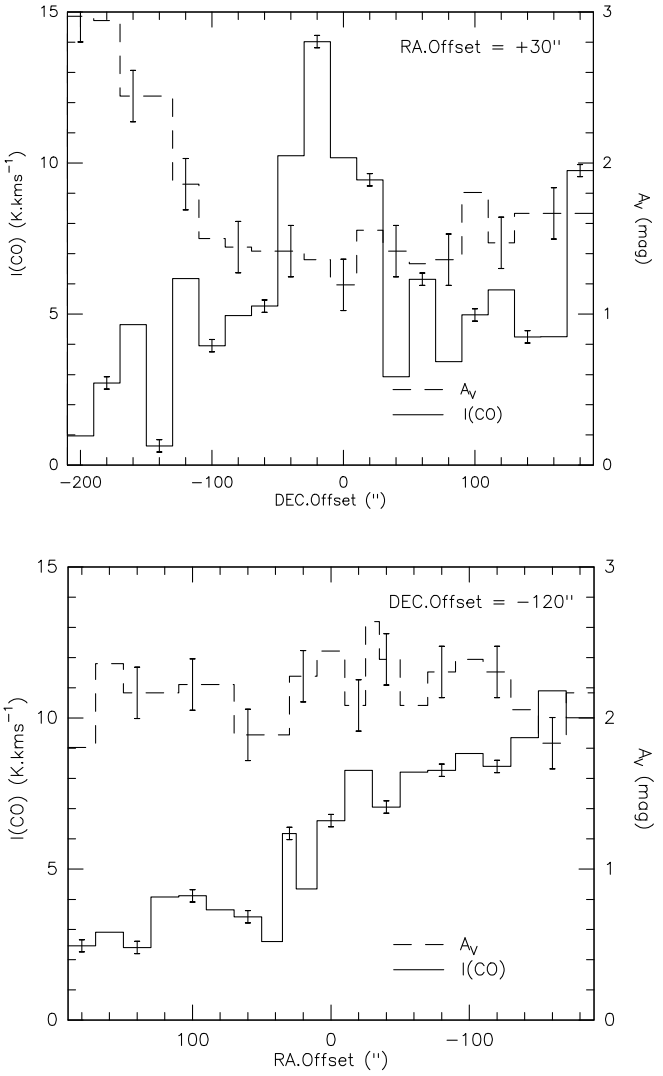


**Fig. 15.** Variation of $I$(CO) (full line) and $A_V$ (dashed line) as a function of position along the two cuts shown in Fig. 13 (a: cut at RA offset = 30″; b: cut at DEC offset = −120″)

the observed CO spectra since we checked that no CO emission is seen at both the "off" and RF positions. The backend used was a 1792 channels autocorrelator with a channel width of 20 kHz, giving a velocity resolution of 0.05 km/s at the $^{12}$CO($J$ = 1–0) frequency. After resampling the channel width to 0.3 km/s, the rms noise in the spectra is lower than 0.15 K. The pointing was checked every two hours on the quasar 0923+392, and was always better than 3″. We observed thirty positions, sampling at 1′ a 6′ × 7′ region roughly covering the CF field (Fig. 12) plus two 6′-long strips at constant R.A. or DEC. and with a spacing of 20″ (Fig. 13). The CO($J$ = 1–0) lines display peak intensities up to 6 K. As for many other clouds, CO($J$ = 2–1) and CO($J$ = 1–0) profiles are identical in shape although several components are present; the ratio of integrated intensities is always close to 0.6.

To correlate CO intensities with visible extinction, we determined $E$(V − i) as described in Sect. 3 but by selecting stars within circular disks centered at the thirty positions observed in the 6′ × 7′ map. A diameter of 40 arcsec was adopted. This size is well matched to the beam in CO($J$ = 1–0) since it is about twice its FWHM. In Fig. 14 we show $I$(CO) versus $A_V$: no correlation can be seen, which can in no way be due to measurement uncertainties. A similar result is obtained for the better sampled E-W and N-S cuts (Fig. 15). Along the former, the extinction is roughly constant within $\delta A_V \approx 0.1$ while $I$(CO) decreases from W to E by a factor of 4 from 10 to 2.5 K km s$^{-1}$. Similarly, along the cut at constant RA, a pronounced maximum is observed for $I$(CO) with an amplitude $\delta I(\mathrm{CO}) \approx 10$ K km s$^{-1}$ while $A_V$ remains nearly constant ($\delta A_V < 0.2$). This complete lack of correspondence between $I$(CO) and $A_V$ can be translated in terms of an upper limit on $X_{CO}$, defined here as $\delta N(\mathrm{H_2})/\delta I(\mathrm{CO})$. From the two E-W and N-S cuts, we get values of 1.3 and 1.0 $10^{19}$ cm$^{-2}$/K km s$^{-1}$ respectively at scales of 40″, i.e. about 30 times lower than the value computed from the average $I$(CO) and $A_V$ over the entire field, $X_{CO} = 2.910^{20}$ cm$^{-2}$/K km s$^{-1}$ (note that this estimate is well compatible with the commonly used value, 2.3 $10^{20}$ cm$^{-2}$/K km s$^{-1}$ given by Bloemen 1989).

## 6. Discussion

### *6.1. The contribution of the diffuse medium*

Dust associated with atomic gas could play a role and tend to weaken the relative fluctuations of the extinction and wash out the correlation between $A_V$ and $I$(CO). The region including CF and RF is within the 21 cm line surveys made at Berkeley (Weaver and Williams 1974). Assuming the line to be optically thin, we find $N$(HI) = 2.5 $10^{21}$ cm$^{-2}$ and 2.4 $10^{21}$ cm$^{-2}$ in CF and RF respectively. We only include emission at velocities larger than −30 km s$^{-1}$ because the rest of the HI lies in distant regions ($d \geq 4$ kpc from Burton 1988) which are not probed by the stars

in CF. The corresponding opacity $A_V$(HI) and opacity difference $\Delta A_V$(HI) = $A_V$(CF) − $A_V$(RF) are 1.3 and 0.05. Since the latter value is quite small, the extinction studied in Sect. 3 is mostly that related to the molecular gas. Indeed, diffuse absorption does not affect our analysis as far as it is the same in the CF and RF fields. Moreover, when comparing the 21 cm spectra towards CF and RF, we find no clear departure around velocities at which CO emission is observed: the amount of HI associated with the cloud should then be small (we could also show in Sect. 4, that in any event, the influence of diffuse extinction at $d \leq 2$ kpc is small). One restriction is that structure in the HI distribution could be present within the large beams used for the observations ($\Delta\theta \approx 0.5$ deg.) (see e.g. Joncas et al. 1992). However, given the low values quoted above for $A_V$ (HI) and $\Delta A_V$ (HI) and given that variations of the 21 cm integrated line intensity appear to be small at a few degrees scale in the region considered, such effects are likely to be unimportant.

### *6.2. The absence of strong extinction fluctuations*

We conclude that all results obtained in Sect. 3 are relevant to the extinction induced by molecular material contained in the cloud. From the analysis of color distributions we could show that dust is spatially distributed in such a way that the resulting fluctuations of the extinction are weak and occur mostly at scales larger than 40 arcsec, i.e. 0.04 pc. Similar results have been obtained for another cloud (Thoraval 1995).

Let us now determine more precisely which constraints can be obtained on the internal structure of the cloud studied. Since we have information only on column densities, we cannot unambiguously relate our observations to the 3D density field inside the cloud. For instance, we cannot say whether the small gradients seen in the color excess map are due to variations in the thickness of the cloud or rather, in its volume density. Nevertheless, one can proceed in the other way and check whether or not a given 3D model leads to expected properties for the associated extinction field which are compatible with the data. For instance, if we consider that extinction is entirely due to clumps smaller than the cell size (and with similar characteristics), we can easily get a lower limit on $N_{cl}$, the average number of fragments intersected by a line of sight through the cloud. In such a model, Poissonian fluctuations are expected with an amplitude $\sigma(A_V)/A_V = 1/\sqrt{N_{cl}}$. Since the latter appears to be locally no larger than about 10%, $N_{cl}$ must be larger than 100, implying that individual clump opacities, $\delta A_V$, are quite small (less than about 0.02). Qualitatively similar conclusions are reached if only some fraction $\alpha$ of the obscuring material is assumed to be in the form of clumps (the rest being distributed uniformly). For $\alpha = 0.5$ or 0.1, one gets $N_{cl} \geq 25$ or 1 and $\delta A_V \leq 0.04$ or 0.2. We see that in any such model, fragments have to be optically thin, a situation equivalent to uniformity regarding radiative transfer.

The weakness of extinction fluctuations is supported by other observations. The study of brightness profiles for galaxies background to molecular clouds confirms in a very direct way that fluctuations of the extinction are quite small beyond the arcsec scale (Thoraval et al. 1997). Further, variability studies have provided stringent upper limits on fluctuations of $A_V$ at AU scales (Thoraval et al. 1996).

These results altogether strongly suggest that no pronounced structure in the dust distribution is "hidden" at scales below those for which imaging or mapping is possible. If we accept that this conclusion is valid for molecular material in general (or at least for translucent and quiescent molecular clouds), one first consequence is that extinction estimates based on star counts have not been strongly biased by structure in count cells. The major systematic errors in the classical procedure are more likely due to the fact that some of the assumptions required are not verified, in particular concerning the absence of curvature for log$N(m)$. To avoid such effects, it is preferable to solve Eqn (5) for each cell (if the shape of $N_r(m)$ could not be determined, a good approximation can be obtained from galactic models; cf the procedure followed by Mattila 1986). Nevertheless, we stress that two-magnitude data allow much more accurate determinations as illustrated in Sect. 3.

One other consequence of our results involves models describing the chemistry of molecular clouds. Since the latter generally assume uniformity, their applicability requires that it is possible to isolate some piece of material inside which the density does not show strong fluctuations. The cloud studied here seems to fulfill this condition since we found $A_{eff}$(UV) ≈ $\langle A(\mathrm{UV})\rangle$. However, we have to be aware of one difficulty: it is not only the extinction along the line of sight which determines the radiation field but the whole cloud morphology (radiation may penetrate more easily from the sides). Unfortunately, there is no direct way to estimate the "transverse" extinction for the region studied. We simply note that we have information over an angular size of about 10 arcmin or 0.6 pc and that a density $n(H_2)$ of about $5\,10^2$ cm$^{-3}$ is required to get $A_V \approx 1$. Such an average value is not unreasonably large and, since the POSS plates show that the cloud field keeps a similar appearance over a still larger extent (≈ 20 arcmin), the region probed may be considered as an "isolated" piece of material which can be modelled as such, assuming uniformity. Hence, when modelling chemistry, structure in the dust distribution may not always be a major problem and other processes, such as time-dependent chemistry, dynamical mixing (Chièze & Pineau des Forêts 1989) or turbulence (Falgarone et al. 1995) should be considered to explain discrepancies between observations and models.

One may wonder to which extent the above conclusions also apply to clouds of higher extinction. Results have been obtained by Lada et al. (1994) on the structure of molecular material much more opaque than the one studied here. Star counts in the J band and H-K colors are used by these authors to map the extinction towards a dark filamentary cloud. They find that in $1.5' \times 1.5'$ cells, the scatter in $A_V$ (derived from H-K colors) increases in a systematic way with the average $A_V$ and attribute this effect to structure within the cells. From their $\sigma(A_V) - A_V$ relation, one can estimate that at $A_V \approx 2.$, the scatter due to structure is $\sigma(A_V) \approx 1.$ mag., a value much larger than what we find in our study over the entire $6' \times 7'$ field. However, there is an important difference between the two regions studied: while we selected a

field which opacity looked well uniform, the extinction across the large area investigated by Lada et al. ranges over a very broad interval ($0 \leq A_V \leq 30$). Then, some fraction of their cells must be located towards regions where steep extinction gradients exist (especially near the boundary of the opaque filament), and this may partly account for the large $\sigma(A_V)$ value observed. The data presented by Lada et al. (1994) could allow to isolate the effect of stochastic fluctuations in high extinction clouds (due e.g. to tiny clumps) by analyzing the behaviour of $\sigma(A_V)$ over regions covering a few adjacent cells and selected for their relatively uniform extinction.

### *6.3. The lack of correlation between $A_V$ and I(CO)*

The cloud we studied appears qualitatively similar to many others in its average $I(CO)/A_V$ and CO spatial variability. However, at the scales we have investigated ($\approx 0.05$ pc) CO emission appears to show a much stronger spatial variability than extinction. This is all the more remarkable since for $A_V$, all scales have been considered whereas for the CO emission, we have access only to the distribution smoothed at a resolution of $22''$. Further, no noticeable correlation appears between the variations of $A_V$ and $I(CO)$, although the uncertainties in both quantities are small. If we accept that dust and gas are well mixed (with the $N(H)/A_V$ ratio given by Bohlin et al. 1978), this lack of relationship implies that CO emission no longer correlates with the $H_2$ column density at scales below about 0.04 pc.

In studying the relation between extinction and CO isotopomers line intensities, authors have generally focussed on the existence of a correlation and payed little attention to the large scatter around the linear fit. Lada et al. (1994) have combined their extinction data covering a broad dynamical range with $^{13}CO$, $C^{18}O$ and CS observations of the same field (at a resolution of 1.7 arcmin) and rediscuss these relations. They show that instrumental uncertainties cannot explain the large scatter observed (as in our Fig. 14) and propose that local variations of either the excitation or abundance of these species are present within the cloud. Similarly large dispersions are observed in $I(^{12}CO)-A_V$ plots (Cernicharo & Guélin 1987). Then, it might seem that since the spread in extinction values is relatively limited in our cloud field, the absence of correlation in Fig. 14 is no surprise. However, it is clear that a relation is much more apparent in the data obtained by Cernicharo & Guélin (1987) at a resolution of 5 arcminutes, as illustrated in Fig. 14 (the difference comes in particular from the regions with large $A_V$ and low CO emission which are absent in the low resolution data). We then conclude that increasing the angular resolution significantly increases the scatter of $I(CO)$ at a given $A_V$. It is likely that if our cloud covered the whole range [0, 3] in $A_V$, we would still see, whatever the angular resolution, some trend in the $I(^{12}CO)-A_V$ plot (no CO emission being expected at $A_V \approx 0$!). The lack of correlation in Fig. 14 may therefore be understood as the result of both an enhanced scatter at higher resolution and a limited dynamical range investigated. At a given $A_V$, $I(CO)$ vary by factors as large as five (Lada et al. 1994 get a similar result for $^{13}CO$ at scales of 1.7 arcmin). Thus, as far as $A_V$ scales linearly with $N(H_2)$, CO emission does not give any information about the detailed variations of the total gaseous column density for the cloud studied here, although the range involved for $A_V$ is such that no strong saturation effects are expected (Cernicharo & Guélin give a linear relation for $0.5 < A_V < 3$).

The above results have implications concerning the origin of the CO emission. Let us consider first models in which the latter arises from the beam- diluted contribution of dense fragments, with $n(H_2) > 10^4\,cm^{-3}$ and a large opacity in the millimeter rotational lines in order to account for the uniformity of line ratios (e.g. Tauber & Goldsmith 1990; Falgarone & Phillips 1996). The spatial variability of the emission is then attributed to a variation in the surface filling factor of these tiny fragments. Since self shielding is more efficient for $H_2$ than for CO because of a larger abundance, it is expected that only part of the $H_2$ is spatially coincident with CO emitting regions. In this frame, the absence of correlation between extinction (i.e. $N(H_2)$) and $I(CO)$ at small scale implies that the $H_2$-rich material lying either inside CO emitting cells or in the immediate vicinity represents a small fraction of the total $H_2$ mass, less than $\approx 10\%$ as derived from the $I(CO)$ and $A_V$ cuts (the remaining 90% of the $H_2$ being uncorrelated to CO). As noted above, both CO and extinction data indicate that the visual extinction per clump must be quite small. It is then not easy to understand how these fragments can survive against photodissociation in the frame of steady-state chemical models. One possibility discussed by Falgarone & Puget (1995) and Falgarone & Phillips (1996) is that CO emission traces the regions of large vorticity where the formation rate may be enhanced by large factors. In such a picture, one does not necessarily expect a detailed relation between $I(CO)$ and total column density, unless the volume density in these singular regions is so large that they enclose a significant fraction of the total mass.

Alternatively, it has been argued that the large spatial variations of $I(CO)$ do not necessarily imply large density variations (Gredel et al. 1992). For translucent clouds like the one studied here, the CO abundance appears to be very sensitive to small variations of the extinction or density (van Dishoeck & Black 1988). We know from our study that small fluctuations of $A_V$ integrated along the line of sight are present but because the full 3D geometry of the cloud is unknown, it is difficult to determine their precise impact on the radiation field and next on the chemistry (roughly speaking, 2 out of 3 "components" of the radiation field remain unknown). When comparing observations to predictions of chemical models, this difficulty is often circumvented by assuming that the cloud consists in a slab viewed face on. In reality, clouds display a complex overall morphology and this assumption is obviously not satisfied in most cases. Then, within a frame in which the CO emitting gas is distributed in a relatively diffuse manner (and ignoring the problems that such a picture may encounter to account for the characteristics of the CO emission), one can imagine that radiation penetrating the cloud along directions perpendicular to the line of sight tends to erase the correlation which would be expected for a slab geometry. As discussed by Thoraval et al. (1996), it is also possible that, due to the complex interplay between time-dependent

chemistry and dynamics (Xie et al. 1995) and/or to chemical bistability (Le Bourlot et al. 1993), the molecular gas never reaches a high degree of homogeneity. These processes have associated time scales of about $10^6$ yr, i.e. much shorter than those characterizing the evolution of dust grains (about $10^9$ yr; Jones et al. 1994) which might explain that some species like CO do not get well mixed to $H_2$ and dust grains.

## 7. Conclusion

In order to probe the small scale spatial distribution of dust grains inside molecular clouds, we have investigated the extinction induced by fragmented clouds on the population of background stars. Estimates of visual extinctions obtained from the classical star count method are found to be quite sensitive to structure and yield only lower limits to the true amount of dust. We have considered one-band magnitude distributions and showed that, provided they clearly depart from an exponential law, the accurate determination of their shape is a powerful tool for quantifying the strength of extinction fluctuations at any scale below the size of the field studied.

Multi-band (B, V, R, i) CCD observations have been performed for a field towards a low latitude translucent ($A_V \approx 1.8$) cloud and a closeby reference field. All one-band magnitude distributions (built from more than one thousand stars) are found to be consistent with a homogeneous structure (with $A_V \approx 1.8$) and exclude strongly fragmented models. The extinctions derived in each band appear to be compatible with known extinction laws, which further supports the previous conclusion.

We have also studied the V − i colors of the background stars and compared them to those observed in the reference field. Because colors are spread over an intrinsically narrow range, the estimate of the additional scatter introduced by the cloud in the values of (reddened) colors provides tight constraints on its structure. We were thus able to model the distribution of the extinction values across the field and found the relative r.m.s. scatter $\sigma(A_V)/A_V$ to be no larger than 25%. By mapping the variations of the V − i color excess in $42 \times 42$ arcsec cells, we have shown that most of the (small) fluctuations can be assigned to scales larger than about $1'$; the accuracy of this color excess method is estimated from Monte-Carlo simulations and some possible biases are discussed. Spectroscopic data obtained for 9 stars are consistent with both the average and dispersion of $A_V$ values over the field obtained from the statistical analysis. Further, we can derive an upper limit to the cloud distance of 200 pc.

High angular $^{12}$CO observations have been performed towards the cloud field. The latter is found to be similar to many other translucent clouds in its strong spatial variability, similarity of $J = 2$–1 and $J = 1$–0 line profiles and uniformity of $J = 2$–1 to $J = 1$–0 integrated line intensity ratio. We compare our accurate ($\sigma(A_V) = 0.17$) high resolution ($42''$ or 0.04 pc) extinction map to the CO data and find no correlation between the spatial variations of $A_V$ and $I$(CO). An upper limit to the ratio $\delta N(H_2)/\delta I(CO)$ of about $10^{19}$ cm$^{-2}$ can be inferred for these small scales.

From these results, we conclude that small scale fluctuations in the distribution of the dust have a too low amplitude to notably affect the penetration of the radiation in such quiescent translucent clouds, even in the UV. The absence of correlation between $I$(CO) and $A_V$ indicates that if CO emission originates from dense fragments with a small volume filling factor, the $H_2$ gas which is associated with (i.e. located inside or just around) these clumps should represent at most 10% of the total $H_2$ mass. Fluctuations of the extinction along directions perpendicular to the line of sight may also tend to wash out the correlation that would be expected in a face-on slab geometry.

*Acknowledgements*. We thank the staff of Observatoire de Haute Provence, Observatoire du Pic du Midi, and 30 m IRAM telescope for their efficient assistance during the observations. We are very grateful to A. Robin who kindly communicated to us results from models of Galactic stellar populations at various stages of this work, to E. Falgarone and M. Gerin for helpful discussions on the origin of the CO emission and to F. Sèvres for measuring optical positions. We also thank the referee, J. Knude for many constructive remarks which helped to clarify the content of this paper. Support provided during the reduction of the data by the Institut d'Astrophysique de Paris (CNRS) have been of great help.

## References

Abergel A., Boulanger F., Mizuno A., Fukui Y., 1994, ApJ 423, L59
Baker P.L., 1976 A&A 50, 327
Bally J. et al., 1987, ApJ 312, L45
Bernard J.P., Boulanger F., Desert X., Puget J.L., 1992, A&A 253, 258
Blitz L., Shu F.H., 1980, ApJ 238, 148
Bloemen H., 1989, ARA&A 27, 469
Bohlin R.C., Savage B.D., Drake J.F., 1978, ApJ 224, 132
Boissé P., 1990, A&A 228, 483
Bok B.J., Cordwell C.S., 1973, In "Molecules in the Galactic Environment", Eds Gordon & Snyder (Wiley, New York)
Boulanger F., Falgarone E., Puget J.L., Helou G., 1990, ApJ 364, 136
Burton W.B., 1988, in Galactic and Extragalactic Radio Astronomy, Eds Verschuur and Kellermann, Springer-Verlag
Cardelli J.A., Clayton G.C., Mathis J.S., 1989, ApJ 345, 245
Cernicharo J., Guélin M., 1987, A&A 176, 299
Chièze J.P., Pineau des Forêts G. 1989, A&A 221, 89
Dickman R.L., 1978, ApJS 37, 407
Dickman R.L., Herbst W.,1990, ApJ 357, 531
Dobashi K., Yonekura Y., Mizuno A., Fukui Y., 1992, AJ 104, 1525
Falgarone E., Phillips T.G., 1996, ApJ (in press)
Falgarone E., Pineau des Forêts G., Roueff E., 1995, A&A 300, 870
Falgarone E., Puget J.L., 1995, A&A 293, 840
Falgarone E., Puget J.L., Pérault M., 1992, A&A, 257, 715
Fasano G., Franceschini A., 1987, MNRAS 225, 155
Franco G.A.P., 1995, A&AS 114, 105
Gautier III T.N., Boulanger F., Pérault M., Puget J.L., 1992, AJ 103 , 1313
Goldsmith P.F., Plambeck R.L., Chiao, R.Y., 1975, ApJ 196, L39
Gredel R., van Dishoeck E.F., de Vries C.P., Black J.H., 1992, A&A 256, 245
Hobson M.P. & Scheuer P.A.G., 1993, MNRAS 264, 145
Jacoby G.H., Hunter D.A., Christian C.A., 1984, ApJS 56, 257
Jønch-Sørensen H., Knude J., 1994, A&A 288, 139

Johnson H.L., 1966, ARAA 4, 193
Joncas G., Boulanger F., Dewdney P.E., 1992, ApJ 397, 165
Jones A.P., Tielens A.G.G.M., Hollenbach D.J., Mc Kee C.F., 1994, ApJ 433, 797
Keene, J., Blake G.A., Phillips T.G., et al, 1985, ApJ 299, 967
Knude J., 1979, A&A 71, 344
Kwan J., Sanders D.B., 1986, ApJ 309, 783
Lada C.J., Lada E.A., Clemens D.P., Bally J., 1994, ApJ 429, 694
Lequeux J., Dantel-Fort M., Fort B., 1995, A&A 296, L13
Le Bourlot J., Pineau des Forêts G., Roueff E., Schilke P., 1993, ApJ 416, L87
Magnani L., Onello J.S., 1995, ApJ 443, 169
Marscher A.P., Bania T.M., Wang Z., 1991, ApJ 371, L77
Marscher A.P., Moore E.M., Bania T.M., 1993, ApJ 419, L101
Martin H.M., Sanders D.B., Hills R.E., 1984, MNRAS 208, 35
Mattila K., 1986, A&A 160, 157
Meixner M., Tielens A.G.G.M., 1993, ApJ 405, 216
Moore E.M., Marscher A.P., 1995, ApJ 452, 671
Natta A., Panagia N., 1984, ApJ 287, 228
Pajot F., Boissé P., Gispert R., et al, 1986, A&A 157, 399
Peacock J.A., 1983, MNRAS 202, 615
Pérault M., Falgarone E., Puget J.L., 1985, A&A 152, 371
Phillips T.G., Huggins, P.J., 1981, ApJ 251, 533
Rossano G.S., 1980 AJ 85 1218
Savage B.D., Mathis J.S.,1979, ARAA 17, 73
Seldner M., Uson J.M., 1983, ApJ 264, 1
Smail I., Hogg D.W., Yan L., Cohen J.G., 1995, ApJ 449, L105
Spaans M., 1996, A&A 307, 271
Stacey G.J., Jaffe D.T., Geis N., et al ,1993, ApJ 404, 219
Stutzki J., Stacey G.J., Genzel R., et al , 1988 , ApJ 332, 379
Stutzki J., Güsten R., 1990, ApJ 356, 513
Tauber J.A., Goldsmith P. F., 1990, ApJ 356, L63
Tauber J.A., Goldsmith P.F., Dickman R.L., 1991, ApJ 375, 635
Tauber J.A., Tielens A.G.G.M., Meixner M., Goldsmith P.F., 1994 ApJ 422, 136
Thoraval S., Boissé P., Stark R., 1996 A&A 312, 973
Thoraval S., 1995, PhD. Thesis
Thoraval et al. 1996, in preparation
van Dishoeck E.F., Black J.H., 1988, ApJ 334, 771
Walker, M.F., 1959, ApJ 130, 57
Weaver H., Williams D.R.W., 1974, A&AS 17, 1
Witt A.N., Gordon K.D., 1996, ApJ 463, 681
Witt A.N., Oliveri M.V., Shield R.E., 1990, AJ 99, 888
Xie T., Allen M., Langer D.W., 1995, ApJ 440, 674
Zaritsky D., 1994, AJ 108, 1619